Studies on the molecular mechanism of the cascade reaction of the three protease zymogens proC, proB, and proCE in the hemolymph coagulation system of horseshoe crabs using their recombinant proteins

山下, 啓介

https://hdl.handle.net/2324/6787440

Studies on the molecular mechanism of the cascade reaction of the three protease zymogens proC, proB, and proCE in the hemolymph coagulation system of horseshoe crabs using their recombinant proteins

Keisuke Yamashita

Graduate School of Systems Life Sciences, Kyushu University

2023

Contents

Part 1

Roles of the clip domains of two protease zymogens in the coagulation cascade in horseshoe crabs

Abbreviations

LPS, lipopolysaccharide

proC, prochelicerase C

proB, prochelicerase B

proCE, the proclotting enzyme

CE, the clotting enzyme

GnTI⁻, lacking *N*-acetylglucosaminyltransferase I

Boc, butoxycarbonyl

MCA, 4-methylcoumaryl-7-amide

SPR, surface plasmon resonance

Hd-PPAF-II, Holotrichia diomphalia prophenoloxidase-activating factor II

Dm-grass, Drosophila melanogaster grass zymogen

Ms-PAP2, Manduca sexta prophenoloxidase activating proteainase-2

SE, standard errors.

Abstract

The lipopolysaccharide (LPS)-triggered coagulation cascade in horseshoe crabs comprises three protease zymogens, prochelicerase C (proC), prochelicerase B (proB), and the proclotting enzyme (proCE). The presence of LPS results in autocatalytic activation of proC to α-chelicerase C, which, in turn, activates proB to chelicerase B, converting proCE to the clotting enzyme (CE). ProB and proCE contain an N-terminal clip domain, but the roles of these domains in this coagulation cascade remain unknown. Here, using recombinant proteins and kinetics and binding assays, we found that five basic residues in the clip domain of proB are required to maintain its LPS-binding activity and activation by α-chelicerase C. Moreover, an amino acid substitution at a potential hydrophobic cavity in proB's clip domain (V55A-proB) reduced both its LPS-binding activity and activation rate. WT proCE exhibited no LPS-binding activity, and the WT chelicerase B–mediated activation of a proCE variant with a substitution at a potential hydrophobic cavity (V53A-proCE) was approximately 4-fold slower than that of WT proCE. The k_{cat}/K_m value of the interaction of WT chelicerase B with V53A-proCE was 7-fold lower than that of the WT chelicerase B-WT proCE interaction. The enzymatic activities of V55A-chelicerase B and V53A-CE against specific peptide substrates were indistinguishable from those of the corresponding WT proteases. In conclusion, the clip domain of proB recruits it to a reaction center composed of α-chelicerase C and LPS, where α-chelicerase C is ready to activate proB, leading to chelicerase B–mediated activation of proCE via its clip domain.

5

Introduction

The horseshoe crab hemolymph contains granular hemocytes, which respond selectively to lipopolysaccharide (LPS) of Gram-negative bacteria by secreting serine protease zymogens to initiate a proteolytic coagulation cascade (1-4). We previously proposed new terms for protease zymogens in the horseshoe crab coagulation cascade—prochelicerase C, prochelicerase B, and prochelicerase G—for factor C, factor B, and factor G, respectively, each of which is activated into the corresponding chelicerase (5). The LPS-triggered horseshoe crab coagulation cascade consists of prochelicerase C (proC), prochelicerase B (proB), and the proclotting enzyme (proCE), all of which belong to the trypsin family.

A classical model for the proteolytic activation of serine protease zymogens has been established for trypsinogen and chymotrypsinogen; both zymogens are activated by proteolytic cleavage of the Arg[15]–Ile[16] bond in chymotrypsinogen numbering, followed by an insertion of the newly appearing N-terminal Ile[16] into the activation pocket, the Ile[16] cleft, to form a salt bridge between the α-amino group of Ile[16] and the side chain of Asp[194], which triggers conformational changes of the substrate binding site and the oxyanion hole required for catalysis (6, 7). On the other hand, studies on autocatalytic activation of two thrombin precursors, prethrombin-2 and prothrombin, have been carried out (8,9). The Arg[15]–Ile[16] bond of prothrombin-2, the immediate precursor of thrombin, is proteolytically cleaved by coagulation factors Xa under physiological conditions, whereas a triple mutant of prethrombin-2 with the E14eA/D14lA/E18A replacements reduces the level of electrostatic interactions between Arg[15] and these residues, which promotes autocatalytic activation of the mutant to the mature enzyme spontaneously without the need for the activation by coagulation factor Xa.

The autocatalytic cleavage of proC in the presence of LPS occurs within the Phe^{737}–Ile^{738} bond, which corresponds to the Arg^{15}–Ile^{16} bond, to produce an active protease α-chelicerae C (3, 4, 10). In the absence of LPS, proC is artificially activated by chymotrypsin through cleavage of the Phe^{737}–Ile^{738} bond with an additional proteolytic cleavage of the Tyr^{40}–Cys^{41} bond, resulting in its conversion into β-chelicerase C with amidase activity against a specific peptide substrate (11). However, β-chelicerase C possesses neither the LPS-binding activity nor the proB-activating activity (11).

The autocatalytic cleavage of proC occurs intermolecularly between proC* (an active transition state) molecules in the presence of LPS (5), and the N-terminal Arg^1 residue of proC is essential for autocatalytic activation (12). The active transition state proC* does not exhibit intrinsic chymotryptic activity against the Phe^{737}–Ile^{738} bond, but it may recognize a three-dimensional structure around the cleavage site (5). The resulting α-chelicerase C activates proB to chelicerase B through proteolytic cleavage of the Ile^{124}–Ile^{125} bond (13), and then chelicerase B converts proCE to the clotting enzyme (CE) through cleavage of the Arg^{98}–Ile^{99} bond (14) (Fig. 1). An LPS-binding site of proC is located in a tripeptide sequence (Arg^{36}–Trp^{37}–Arg^{38}) in the N-terminal cysteine-rich domain with a dissociation constant of (K_d) = 7.6×10^{-10} M (15).

Instead of the N-terminal cysteine-rich domain in proC, proB and proCE contain an N-terminal clip domain (13, 14). The clip domain was first identified in proCE (14); later, clip-domain-containing proteases or protease homologs were identified in arthropods, such as those involved in dorsal-ventral polarity in *Drosophila* and the proteolytic cascades of prophenoloxidase in insects (16-22). These clip domains are characterized by six strictly conserved cysteine residues that form three disulfide bridges (14). The clip-domain-containing proteases are proteolytically activated by their specific upstream proteases, and the clip and catalytic domains of the resulting active forms remain to be covalently linked by a disulfide bond

(14). However, roles of the clip domains of proB and proCE in the coagulation cascade remain unknown. Interestingly, proB binds to LPS and a mutant proB without the clip domain (Δclip-proB) decreases its LPS-binding activity and exhibits lower activation rate by α-chelicerase C than WT proB (11).

In this study, to examine the roles of the clip domains of proB and proCE, we prepared several variants of proB and proCE with mutants in the clip domains, and compared the LPS-binding activity and the activation rate of each of the mutants with those of the WT zymogens. On the other hand, a reagent prepared from hemocyte lysates of horseshoe crabs has been used for the "*Limulus* test", a sensitivity test to detect LPS (23, 24). Here we prepared a WT proCE to apply a functional recombinant zymogen to a next-generation *Limulus* test.

Results

The proteolytic activation of proB was quantified by Western blotting

The WT proB, prepared in an HEK293S cell line lacking *N*-acetylglucosaminyltransferase I (GnTI⁻), contains two types of zymogen; the single-chain form and the two-chain form, consisting of the H and L chains formed through cleavage at site 1 by an unknown protease (Fig. 1). The activation rate of both types of proB by α-chelicerase C is followed by appearance of the B chain through the cleavage at site 2 by Western blotting using an anti-B chain antibody (11).

To confirm whether the cleavage reaction at site 2 for the proteolytic activation was quantified by Western blotting, WT proB at varying concentrations was incubated with α-chelicerase C in the presence of LPS at [E]/[S] = 1/200 for 30 min at 37°C and subjected to Western blotting. Site 2 of WT proB was cleaved and the resulting B chain was detected (Fig. 2A). The relative band density was in direct proportion to the concentration of WT proB at least in the density range between 25 and 100 nM (Fig. 2B). After 30-min of incubation, WT proB at every concentration was cleaved ~35% under the conditions used (Fig. 2C).

Basic residues in the clip domain of proB are required to maintain the activation rate by α-chelicerase C

Studies on LPS-binding proteins, such as proC (14), horseshoe crab anti-LPS factor (25), human MD2 (26, 27), and mammalian caspase-4/5/11 (28) demonstrated that specific basic residues in their amino acid sequences are required for the interaction with LPS. The clip domain of proB contains five basic residues (Arg[17], Lys[21], Lys[25], Lys[38], and Arg[50]). To determine whether the basic residues in the clip domain of proB are involved in the interaction with LPS, substitution mutants

were prepared by replacing each of these basic residues with a glutamic acid, R17E-proB, K21E-proB, K25E-proB, K38E-proB, and R50E-proB.

Each of these substitution mutants was incubated with WT α-chelicerase C in the presence of LPS and subjected to Western blotting (Fig. 3A). All of the mutants, especially K21E-proB, K25E-proB, and K38E-proB, exhibited slower activation rates by α-chelicerase C at the initial reaction phase around ~2-min incubation than WT proB (Fig. 3A and 3B). To confirm the reduction of the activation rates of K21E-proB, K25E-proB, and K38E-proB by Western blotting, the expression time-course of the amidase activity was monitored using a fluorogenic peptide substrate for chelicerase B, butoxycarbonyl (Boc)-L-T-R-4-methylcoumaryl-7-amide (MCA). The amidase activities of the three mutants were expressed more slowly than that that of WT proB (Fig. 3C). These findings indicate that the basic residues in the clip domain of proB play important roles to maintain the activation rate by α-chelicerase C.

The basic residues in the Clip domain of proB are required to maintain the LPS-binding activity of proB

To determine the LPS-binding activity of these mutants of proB, the LPS-binding parameters were determined by surface plasmon resonance (SPR) analysis. As a positive control, WT proB exhibited an LPS-binding activity with a dissociation constant of $K_d = 1.2 \times 10^{-9}$ M ($k_{ass} = 6.0 \times 10^5$ M^{-1}s^{-1} and $k_{diss} = 7.6 \times 10^{-3}$ s^{-1}), comparable to the reported value of $K_d = 3.5 \times 10^{-9}$ M (11). However, the binding parameters of the five point mutants of proB could not be determined by SRP analysis because of their lower affinity to LPS coated on the sensor tip. These findings indicate that the basic residues in the clip domain of proB play an important role in maintaining the LPS-binding activity.

Determination of kinetic parameters for the activated forms of K21E-proB, K25E-proB, and K38E-proB against the peptide substrate Boc-L-T-R-MCA

K21E-proB, K25E-proB, and K38E-proB, were fully converted into the active forms, which required 6-h incubation at 37°C with WT α-chelicerase C in the presence of LPS, and the kinetic parameters were determined using the specific fluorogenic substrate, Boc-L-T-R-MCA. A preliminary experiment using WT chelicerase B showed a very large K_m value (~200 μM). Therefore, only k_{cat}/K_m values were determined under the conditions of [S] < K_m at the enzyme concentration of 10 nM, as described in the section *Experimental Procedures*.

The k_{cat}/K_m values of these activated mutants were equivalent to that of WT chelicerase B (Table 1), indicating that the substitutions of Lys[21], Lys[25], and Lys[38] with Glu did not affect the amidase activities against the peptide substrate.

A potential hydrophobic cavity in the clip domain of proB is required to maintain the activation rate by α-chelicerase C and the LPS-binding activity of proB

Crystal structural analyses of the clip domains in insects were reported for prophenoloxidase-activating factor II (*Hd*-PPAF-II) of the beetle *Holotrichia diomphalia* (29), grass protease zymogen (*Dm*-grass) of the fly *Drosophila melanogaster* (30), and prophenoloxidase activating proteainase-2 (*Ms*-PAP2) of the moth *Manduca sexta* (31). These analyses revealed a unique hydrophobic cavity in the clip domains, comprising several conserved hydrophobic amino acids (*dots* in Fig. 4A).

The hydrophobic cavity of *Hd*-PPAF-II is very important for recognizing prophenoloxidase, because an *Hd*-PPAF-II mutant with a substitution of V111A causes a deficiency of the cofactor activity needed for the proteolytic activation of prophenoloxidase (29). Therefore, we prepared a substitution mutant in the clip domain of proB (V55A-proB), which corresponds to the Val[111]

residue of *Hd*-PPAF-II (Fig. 4A). Based on the sequence similarity, the locations of V-55 and the five basic residues in the clip domain of proB were superimposed in the crystal structure of the clip domain of *Hd*-PPAF-II (Fig. 4B).

The activation of V55A-proB by WT α-chelicerase C in the presence of LPS was monitored by both Western blotting and the expression time course of the amidase activity. Western blotting indicated that the relative band intensity of the B chain for V55A-proB at 5-min incubation was 4-fold lower than that for WT proB (Fig. 5, A and B). The expression of the amidase activity for V55A-proB at 5-min incubation was 6-fold lower than that for WT proB (Fig. 5C).

V55A-proB was fully converted into V55A-chelicerase B by 6-h incubation with WT α-chelicerase C in the presence of LPS. The k_{cat}/K_m value of V55A-chelicerase B against Boc-L-T-R-MCA was equivalent to that of WT chelicerase B, suggesting that the potential hydrophobic cavity of proB does not affect the amidase activity (Table 1).

Interestingly, V55A-proB exhibited no binding activity against the LPS-coated tip of the SRP sensor, indicating that the potential hydrophobic cavity plays a role in maintaining the LPS-binding activity of proB.

Preparation of WT proCE and the LPS-binding assay of WT proCE by SPR analysis

ProCE is another clip-domain-containing zymogen in the coagulation cascade. Native proCE purified from horseshoe crab hemocytes is a single-chain glycoprotein with an apparent molecular mass of 54 kDa on SDS-PAGE (14, 32). In the present study, WT proCE was prepared in the HEK293S GnTI⁻ cells, which produces recombinants with a restricted and homogeneous *N*-glycan of $Man_5GlcNAc_2$ (33). The prepared WT proCE had a single band with an apparent molecular mass of 48 kDa on SDS-PAGE (Fig. 6A).

WT proCE had no significant affinity against the LPS-coated tip of the SPR sensor, indicating that the clip domain of proCE has no LPS-binding activity. The LPS-dependent autocatalytic activation of proC is inhibited by Triton X-100 above the critical micelle concentration at 0.24 mM (12). To examine the effect of Triton X-100 on the activation of proCE by chelicerase B in the presence of LPS, Triton X-100 was added to the reaction mixture of WT proCE (50 nM) and WT chelicerase B (1.3 nM) in the presence of LPS (10 nM). Triton X-100 at 0.8 mM did not inhibit the activation of WT proCE under the conditions used, suggesting that LPS is not a requirement for the proteolytic activation of proCE by chelicerase B.

The potential hydrophobic cavity in the clip domain of proCE is required to maintain the activation rate by chelicerase B

WT proCE was incubated at 37°C with WT chelicerase B at [E]/[S] = 1/17, and the time course of the proteolytic conversion of proCE to CE was evaluated by the appearance of the H chain on Western blotting using anti-H-chain antibody. WT proCE was almost fully converted to WT CE by 15-min incubation under the conditions used (Fig. 6B, *left panel*). To examine whether the clip domain of proCE plays an important role in the activation by chelicerase B, we prepared a deletion mutant of the clip domain, Δclip-proCE. The relative band intensity of H chain for Δclip-proCE at 5-min incubation was 3-fold lower than that for WT proCE (Fig. 6B, *middle panel* and Fig. 6C). To confirm the reduction of the activation rate of Δclip-proCE by WT chelicerase B, the expression time-course of the amidase activity was monitored using a specific peptide substrate, Boc-L-G-R-MCA, indicating that the activation rate of Δclip-proCE was approximately 7-fold slower than that of WT proCE (Fig. 6D).

We prepared a substitution mutant of V53A in the clip domain of proCE (V53A-proCE), which corresponds to Val[55] of proB, the component of the potential hydrophobic cavity. The time

13

course of the conversion of V53A-proCE to V53A-CE was also evaluated by both Western blotting (Fig. 6B, *right panel* and Fig. 6C) and the amidase activity against the specific peptide substrate (Fig. 6D). Based on the expression of amidase activity for the resulting V53A-CE, the proteolytic conversion rate observed for V53A-proCE was approximately 4-fold slower than that observed for WT proCE (Fig. 6D), indicating that the potential hydrophobic cavity of proCE is required to maintain the activation rate by chelicerase B.

Determination of kinetic parameters for WT CE, Δclip-CE, and V53A-CE against the peptide substrate Boc-L-G-R-MCA

WT proCE was fully converted into WT CE by 1-h incubation with WT chelicerase B. On the other hand, Δclip-proCE and V53A-proCE were fully converted into the activated forms by 2-h incubation with WT chelicerase B. The kinetic parameters were determined using Boc-L-G-R-MCA. A preliminary experiment showed that the K_m value of WT CE was ~50 μM, and therefore, the substrate concentrations between 6.25 μM and 100 μM were used at the enzyme concentration of 50 pM. The K_m and k_{cat} values of Δclip-CE and V53A-CE were comparable to those of WT CE (Table 1). These results indicate that the clip domain of CE has no effect on the amidase activity against the peptide substrate.

It is noteworthy that the amidase activity of WT CE against the fluorogenic substrate was higher than those of other proteases in the horseshoe crab coagulation cascade; the k_{cat}/K_m value of WT CE was approximately 10-fold and 700-fold higher than those of WT α-chelicerase C (12) and WT chelicerase B (Table 1) against their specific synthetic substrates, respectively.

Determination of kinetic parameters for WT chelicerase B against two protein substrates, WT

proCE and V53A-proCE

The kinetic parameters for WT chelicerase B were determined against WT proCE and V53A-proCE, as described in the section ***Experimental Procedures***. The K_m value of WT chelicerase B against V53A-proCE was 1.8-fold higher than that against WT proCE, and the kcat value of WT chelicerase B against V53A-proCE was 4-fold lower than that against WT proCE (Table 2). Consequently, a 7-fold decrease was calculated in the k_{cat}/K_m value against V53A-proCE, compared to that against WT proCE. These results indicate that the clip domain of proCE is important to enhance the *ES* complex formation and to increase the catalytic turnover number of chelicerase B.

Discussion

The LPS-binding site in the N-terminal cysteine-rich region of proC contains the tripeptide sequence with an aromatic residue immediately flanked by two basic residues (Arg[36]–Trp[37]–Arg[38]) (15), and this motif appears in other LPS-binding proteins, such as human bactericidal permeability-increasing protein (34) and *Limulus* anti-LPS factor (25, 35). The substitution mutants R36E/R38E-proC and W37A-proC, result in the loss of LPS-binding activity of proC (15). Therefore, in the LPS-binding model of proC, the basic side chains of Arg[36] and Arg[38] interact with the phosphates in the lipid A portion of LPS, and the hydrophobic side chain of Trp[37] stacks a hydrophobic surface of the pyranose ring of the glucosamine in the lipid A molecule through the π-π interaction (15).

The substitution mutants at the five basic residues and the Val[55] residue in the clip domain of proB caused the loss of the LPS-binding activity, as assessed by SPR analysis. The basic residues, such as Lys[21], Lys[25] and Arg[50], were estimated to be three-dimensionally located on either side of the hydrophobic Val[55] residue (Fig. 4B). Therefore, the clip domain of proB may have a similar structural strategy to bind to the lipid A molecule of LPS. However, in this study, each of the five basic residues of proB—i.e., Arg[17], Lys[21], Lys[25], Lys[38], and Arg[50]—was replaced to the Glu residue, resulting in the opposite charge at the substitution site, which may have had different effects on the functional activities, compared to the Ala replacement.

Based on SPR analysis, WT proCE exhibited no LPS-binding activity. Interestingly, three of the five basic residues required for LPS-binding in proB, Lys[21], Lys[38] and Arg[50], are replaced to Glu[18], Asn[37], and Gly[48], respectively, in proCE (Fig. 4A). These substitutions possibly reflect a characteristic of the clip domain of proCE with no LPS-binding activity. V55A-proB

16

resulted in a reduction of the activation rate by α-chelicerase C (Fig. 5, A and B), and V53A-proCE also reduced the activation rate by chelicerase B, compared to that of the WT proCE (Fig. 6). Moreover, the k_{cat}/K_m value of WT chelicerase B against V53A-proCE was 7-fold lower than that against WT proCE (Table 2). These findings suggest that the potential hydrophobic cavity of the clip domain of proB or proCE functions in proteolytic activation by the corresponding upstream protease in the coagulation cascade, possibly by enhancing the formation of a favorable *ES* complex between α-chelicerase C and proB or between chelicerase B and proCE and also by increasing the catalytic turnover numbers of α-chelicerase C and chelicerase B. The clip domain of the protease zymogen *Hd*-PPAF-I is also reported to have an essential role in its rapid activation (29).

The kinetic parameters of the amidase activity of the activated mutants, including K21E-chelicerase B, K25E-chelicerase B, K38E-chelicerase B, V55A-chelicerase B, V53A-CE, and Δclip-CE, were equivalent to those of the corresponding WT enzymes (Table 1), indicating that the clip domains of chelicerase B and CE do not affect their catalytic efficiency against the peptide substrates.

Fig. 7 shows a proposed model for the roles of the clip domains of proB and proCE in the coagulation cascade. ProC forms a homo-oligomer in the presence of LPS (15), and the N-terminal Arg and the distance between the N terminus and the tripeptide motif are essential elements for the oligomer formation (12). The resulting oligomer of proC is converted into the active transition state of proC*, leading to autocatalytic conversion into α-chelicerase C (5). ProB is recruited to a reaction center composed of α-chelicerase C and LPS through the clip domain of proB to produce chelicerase B. Then, the potential hydrophobic cavity in the clip domain of proCE accelerates the *ES* complex formation between chelicerase B and proCE to produce CE, thereby promoting hemolymph coagulation. Therefore, the clip domains of proB and proCE play essential

roles in the zymogen-LPS or the protease-substrate interaction to control the activation of the coagulation cascade in response to infection by Gram-negative bacteria at local sites of injury. WT proC (12) and proB (11) expressed in the HEK293S GnTI⁻ cells exhibit procoagulant activities equivalent to those of native proC and proB. In the present study, we prepared WT proCE expressed in the same cell line. WT proCE was fully converted into the active form by WT chelicerase B (Fig. 6). The kinetic parameters of the resulting WT CE against the specific peptide substrate demonstrated an extremely high amidase activity compared to those of WT α-chelicerase C and WT chelicerase B (Table 1). We conclude that WT proCE with high procoagulant activity was successfully prepared.

Therefore, the three recombinant protease zymogens in the LPS-triggered coagulation cascade, consisting of proC, proB, and proCE, could be applied to a next generation of the *Limulus* test to contribute to the development of sensitive and convenient assays for the detection of LPS for a variety of biomedical uses. These recombinant coagulation factors will also help to reduce the use of native ones prepared from hemocytes of the endangered horseshoe crabs.

Experimental procedures

Materials

HEK293S GnTI⁻ cells were obtained from ATCC. LPS derived from *Salmonella Minnesota* R595 (Re) was purchased from List Biological Laboratories, Inc. (Campbell, CA) and used for proB and proCE activation assays. An average molecular weight of 2,500 for R595 (Re) LPS was used for determination of the molar concentration. Biotinylated LPS derived from *Escherichia coli* O111:B4 was purchased from InvivoGen (San Diego, CA) and used in the SPR analysis for the determination of binding parameters. Peptide substrates were purchased from Peptide Institute, Inc. (Osaka, Japan).

Cloning and mutagenesis of proB and proCE

Full-length DNA fragments of proB and proCE derived from the horseshoe crab *Tachypleus tridentatus* were subcloned into vector pCA7 (13, 36, 37), and a sequence derived from pHLsec was used as a secretion signal sequence (38). A His-tag was added to the C-terminal end of proB by site-directed mutagenesis using inverse PCR. A His-tag and a cleavage site of PreScission protease were added to the N-terminal end of proCE by site-directed mutagenesis using inverse PCR. To prepare Δclip-proCE, the full-length proCE contained the cleavage site for PreScission protease between the clip domain and linker region (the Pro^{56}–Lys^{57} bond).

Expression and purification of recombinant proteins

Recombinant proteins of proC, proB, proCE, proB mutants, and proCE mutants were expressed and purified as described previously (11). In brief, culture media containing recombinant proteins

19

were mixed with 0.1 volumes of 0.5 M NaH$_2$PO$_4$-NaOH, pH 8.0, containing 1.5 M NaCl and 0.1

M imidazole, and applied to a Ni-NTA-agarose column (1.0 × 10 cm). The column was washed

with 50 mM NaH$_2$PO$_4$-NaOH, pH 8.0, containing 150 mM NaCl and 10 mM imidazole, and the

recombinant proteins were eluted with 20 mM Tris-HCl, pH 8.0, containing 150 mM NaCl and

50-200 mM imidazole. The N-terminal region containing the His-tag and the clip domain of

proCE was cut off by PreScission protease. The resulting samples were exchanged with 20 mM

Tris-HCl, pH 8.0, containing 150 mM NaCl. The concentrations of recombinant proteins were

determined using a Micro BCA™ protein assay kit (Thermo Scientific).

Activation of WT proB and proB mutants

WT proC (200 nM) was autocatalytically activated in the presence of LPS (8.0 μM) for 30 min at

37°C. The resulting WT α-chelicerase C was diluted with 20 mM Tris-HCl, pH 8.0, containing

150 mM and NaCl. WT proB and proB mutants (100 ~ 150 nM) were activated by WT α-

chelicerase C (1.0 ~ 1.5 nM) in 20 mM Tris-HCl, pH 8.0, containing 150 mM NaCl at 37°C in

the presence of LPS (40 ~ 60 nM). The amidase activities of aliquots at the indicated times were

determined by incubation with 0.4 mM Boc-L-T-R-MCA for 5 min at 37°C, and 10% acetic acid

was added to terminate the reaction. The rate of substrate hydrolysis was measured

fluorometrically with excitation at 380 nm and emission at 440 nm (39).

Activation of WT proCE and proCE mutants

WT proB (6.0 nM) was activated by WT α-chelicerase C (0.3 nM) in 20 mM Tris-HCl, pH 8.0,

containing 150 mM NaCl for 15 min at 37°C in the presence of LPS (12 nM). The resulting WT

chelicerase B (3.0 nM) was incubated with WT proCE or proCE mutants (50 nM). The amidase

activities of the aliquots at the indicated times were assayed with 0.4 mM Boc-L-G-R-MCA as

described in subsection Activation of WT proB and proB mutants.

Western blotting

Samples were subjected to SDS-PAGE in 12% slab gel and transferred to a PVDF membrane. After blocking with 5% skim milk, the membrane was incubated at room temperature for 1 h with polyclonal antibody against the B-chain of chelicerase B (11) or the H-chain of CE (40) and then with the secondary antibody (HRP-conjugated goat anti-rabbit IgG; Bio-Rad), followed by development with Western Bright Sirius or ECL (Advansta, Menlo Park, CA).

Kinetic analysis of WT α-chelicerase, WT chelicerase B, WT CE, and the mutants of chelicerase B and CE against peptide substrates

Proteases including WT α-chelicerase C, WT chelicerase B, WT CE, and the mutants of chelicerase B and CE were incubated with their specific MCA substrates at 37°C in 20 mM Tris-HCl, pH 8.0, containing 150 mM NaCl and 0.1 mg/ml of bovine serum albumin. The initial rate of hydrolysis was measured fluorometrically with excitation at 380 nm and emission at 440 nm after adding the substrate solution. A kinetic parameter (k_{cat}/K_m) for WT chelicerase B or the mutants of chelicerase B was determined under the concentrations of $[S] < K_m$ ($[S] = 12.5$ μM, 25 μM, and 50 μM) at the enzyme concentration of 10 nM. When these conditions were used, the Michaelis-Menten equation $v = k_{cat}[E]_t[S] / (K_m + [S])$ reduces to $k_{cat}/K_m = v/[E]_t[S]$, since the sum total of $K_m + [S]$ was almost equal to K_m (41). On the other hand, kinetic parameters for WT α-chelicerase C, WT CE or the mutants of CE were determined by direct linear plotting (42) using the substrate concentrations of 12.5 μM, 25 μM, 50 μM, 100 μM, and 150 μM for WT α-chelicerase C at the enzyme concentration of 2 nM and those of 6.25 μM, 12.5 μM, 25 μM, 50 μM, and 100 μM for CE or the mutants of CE at the enzyme concentration of 50 pM.

Kinetic analysis of WT chelicerase B against two protein substrates, WT ProCE and V53A-proCE

WT chelicerase B was incubated with WT proCE or V53-proCE at 37°C in a cuvette of a spectrofluorometer containing 20 mM Tris-HCl, pH 8.0, 150 mM NaCl, 0.1 mg/ml of bovine serum albumin, and 200 μM of Boc-L-G-R-MCA, the specific peptide substrate for CE. The hydrolysis of the peptide substrate by the resulting WT CE or V53A-CE was measured continuously, and the rates of the hydrolysis of the peptide substrate were calculated by tangential velocities of the hydrolysis curves. The concentrations of WT CE and V53A-CE converted from the corresponding zymogens by WT chelicerase B were calculated using the k_{cat} value of WT CE or V53A-CE as follows. Under the conditions of [S = Boc-L-G-R-MCA] > K_m (the K_m value of E = WT CE or V53A-CE against the peptide substrate were ~50 μM as shown in Table 1), v = $k_{cat}[E]_t[S] / (K_m + [S])$ reduces to $v = k_{cat}[E]_t$, since the sum total of $K_m + [S]$ was almost equal to [S] (41). [E]$_t$, equal to [WT CE or V53A-CE], was calculated using their kcat values. Kinetic parameters for WT chelicerase B against WT proCE and V53A-proCE were determined by direct linear plotting (42) using the protein substrate concentrations of 100 nM, 150 nM, 200 nM, 300 nM, and 400 nM at the enzyme concentration of 1.0 nM.

Statistical analysis

Statistical analysis was performed by unpaired *t*-tests. *P*-values < 0.05 were considered to be statistically significant.

LPS-binding assay with SPR analysis

Biotinylated LPS (0.1 μg) in 20 mM Tris-HCl, pH 8.0, containing 150 mM NaCl was immobilized

on a sensor chip SA of a BIAcore X system (GE Healthcare), according to the manufacturer's specifications. Recombinant proteins were injected at a flow rate of 30 μl/min in the running buffer, 20 mM Tris-HCl, pH 8.0, containing 150 mM NaCl. The change in the mass concentration on the sensor chip was monitored as a resonance signal by using the program supplied by the manufacturer. Sensorgrams of the interactions obtained by using the various concentrations of recombinant proteins (10 ~ 100 nM) were analyzed by the BIAEVALUATION program, version 3.0.

Reference

1. Toh, Y., Mizutani, A., Tokunaga, F., Muta, T., and Iwanaga, S. (1991) Morphology of the granular hemocytes of the Japanese horseshoe crab *Tachypleus tridentatus* and immunocytochemical localization of clotting factors and antimicrobial substances. *Cell Tissue Res*. **266**, 137–147

2. Ariki, S., Koori, K., Osaki, T., Motoyama, K., Inamori, K., and Kawabata, S. (2004) A serine protease zymogen functions as a pattern-recognition receptor for lipopolysaccharides. *Proc. Natl. Acad. Sci. U. S. A*. **101,** 953–958

3. Kawabata, S. and Muta, T. (2010) Sadaaki Iwanaga: discovery of the lipopolysaccharide- and β-1, 3-D-glucan-mediated proteolytic cascade and unique proteins in invertebrate immunity. *J. Biochem.* **147**, 611–618

4. Kawabata, S. (2010) Immunocompetent molecules and their response network in horseshoe crabs. In *Invertebrate Immunity* (Söderhäll, K., ed) pp. 122–136, Springer Science + Business Media, New York, NY

5. Shibata, T., Kobayashi, Y., Ikeda, Y., and Kawabata, S. (2018) Intermolecular autocatalytic activation of serine protease zymogen factor C through an active transition state responding to lipopolysaccharide. *J. Biol. Chem*. **293**, 11589–11599

6. Bode, W., and Huber, R. (1976) Induction of the bovine trypsinogen—trypsin transition by peptides sequentially similar to the N-terminus of trypsin. *FEBS Lett.* **68**, 231–236

7. Huber, R., and Bode, W. (1978) Structural basis of the activation and action of trypsin. *Acc. Chem. Res.* 11, 114–122

8. Pozzi, N., Chen, Z., Zapata, F., Pelc, L. A., Barranco-Medina S., and Di Cera, E. (2011) Crystal

structures of prothrombin-2 reveal alternative conformations under identical solution conditions and the mechanism of zymogen activation. *Biochemistry* **50**, 10195–10202

9. Pozzi, N., Chen, Z., Zapata, F., Niu, W., Barranco-Medina, S., Pelc, L. A., and Di Cera E. (2013) Autoactivation of thrombin precursors. *J. Biol. Chem*. **288**, 11601–11610

10. Nakamura, T., Morita, T., and Iwanaga, S. (1986) Lipopolysaccharide-sensitive serine-protease zymogen (factor C) found in *Limulus* hemocytes. Isolation and characterization. *Eur. J. Biochem.* **154,** 511–521

11. Kobayashi, Y., Takahashi, T., Shibata, T., Ikeda, S., Koshiba, T., Mizumura, H., Oda, T., and Kawabata, S. (2015) Factor B is the second lipopolysaccharide-binding protease zymogen in the horseshoe crab coagulation cascade. *J. Biol. Chem.* **290,** 19379–19386

12. Kobayashi, Y., Shiga, T., Shibata, T., Sako, M., Maenaka, K., Koshiba, T., Mizumura, H., Oda, T., and Kawabata, S. (2014) The N-terminal Arg residue is essential for autocatalytic activation of a lipopolysaccharide-responsive protease zymogen. *J. Biol. Chem.* **289,** 25987–25995

13. Muta, T., Oda, T., and Iwanaga, S. (1993) Horseshoe crab coagulation factor B. A unique serine protease zymogen activated by cleavage of an Ile-Ile bond. *J. Biol. Chem.* **268,** 21384–21388

14. Muta, T., Hashimoto, R., Miyata, T., Nishimura, H., Toh, Y., and Iwanaga, S. (1990) Proclotting enzyme from horseshoe crab hemocytes. cDNA cloning, disulfide locations, and subcellular localization. *J. Biol. Chem.* **265,** 22426–22433

15. Koshiba, T., Hashii, T., and Kawabata, S. (2007) A structural perspective on the interaction between lipopolysaccharide and factor C, a receptor involved in recognition of Gram-negative bacteria. *J. Biol. Chem.* **282,** 3962–3967

16. Anderson, K. V. (1998) Pinning down positional information: dorsal–ventral polarity in the *Drosophila* embryo. *Cell.* **95,** 439–442

17. Ashida, M and Brey, P. T. (1997) Recent advances in research on the insect prophenoloxidase cascade. In *Molecular Mechanism of Immune Responses in Insects* (Brey, P. T. and Hultmark, D., eds) pp. 135–172, Chapman and Hall, London

18. Lee, S. Y., Cho, M. Y., Hyun, J. H., Lee, K. M., Homma, K., Natori, S., Kawabata, S., Iwanaga, S., and Lee, B. L. (1998) Molecular cloning of cDNA for pro-phenol-oxidase-activating factor I, a serine protease is induced by lipopolysaccharide or 1, 3-*β*-glucan in coleopteran insect, *Holotrichia diomphalia* larvae. *Eur. J. Biochem.* **257,** 615–621

19. Jiang, H. and Kanost, M. R. (2000) The clip-domain family of serine proteinases in arthropods. *Insect Biochem. Mol. Biol.* **30,** 95–105

20. Cerenius, L. and Söderhäll, K. (2004) The prophenoloxidase-activating system in invertebrates. *Immunol. Rev.* **198,** 116–126

21. Volz, J., Osta, M. A., Kafatos, F. C., and Müller, H. (2005) The roles of two clip domain serine proteases in innate immune responses of the malaria vector *Anopheles gambiae. J. Biol. Chem.* **280,** 40161–40168

22. Veillard, F., Troxler, L., and Reichhart, J. M. (2016) *Drosophila melanogaster* clip-domain serine proteases: Structure, function and regulation. *Biochimie.* **122,** 255–269

23. Armstrong, P. B. (2003) Internal defense against pathogenic invasion: the immune system. In *The American Horseshoe Crab* (Shusetr, C. N., Barlow, R. B., and Brockmann, H. J., eds) pp. 288–309, Harvard University Press, Cambridge, MA

24. Levin, J., Hochstein, H. D., and Novitsky, T., J. (2003) Clotting cells and *Limulus* amebocyte lysate: an amazing analytical tool. In *The American Horseshoe Crab* (Shusetr, C. N., Barlow, R. B., and Brockmann, H. J., eds) pp. 310–340, Harvard University Press,

Cambridge, MA

25. Aketagawa, J., Miyata, T., Ohtsubo, S., Nakamura, T., Morita, T., Hayashida, H., Miyata, T., Iwanaga, S., Takao, T., and Shimonishi, Y. (1986) Primary structure of Limulus anticoagulant anti-lipopolysaccharide factor. *J. Biol. Chem.*, 261, 7357–7365

26. Ohto, U., Fukase, K., Miyake, K., and Satow, Y. (2007) Crystal structures of human MD-2 and its complex with antiendotoxic lipid IVa. *Science.* **316,** 1632–1634

27. Park, B. S., Song, D. H., Kim, H. M., Choi, B., Lee, H., and Lee, J. (2009) The structural basis of lipopolysaccharide recognition by the TLR4–MD-2 complex. *Nature.* **458,** 1191–1195

28. Shi, J., Zhao, Y., Wang, Y., Gao, W., Ding, J., Li, P., Hu, L., and Shao, F. (2014) Inflammatory caspases are innate immune receptors for intracellular LPS. *Nature.* **514,** 187–192

29. Piao, S., Song, Y., Kim, J. H., Park, S. Y., Park, J. W., Lee, B. L., Oh, B., and Ha, N. (2005) Crystal structure of a clip-domain serine protease and functional roles of the clip domains. *EMBO J.* **24,** 4404–4414

30. Kellenberger, C., Leone, P., Coquet, L., Jouenne, T., Reichhart, J. M., and Roussel, A. (2011) Structure-function analysis of grass clip serine protease involved in *Drosophila* Toll pathway activation. *J. Biol. Chem.* **286,** 12300–12307

31. Huang, R., Lu, Z., Dai, H., Velde, D. V., Prakash, O., and Jiang, H. (2007) The solution structure of clip domains from *Manduca sexta* prophenoloxidase activating proteinase-2. *Biochemistry.* **46,** 11431–11439

32. Nakamura, T., Morita, T., and Iwanaga, S. (1985) Intracellular proclotting enzyme in *Limulus* (*Tachypleus tridentatus*) hemocytes: its purification and propertied. *J. Biochem.* **97,** 1561–1574

33. Reeves, P. J., Callewaert, N., Contreras, R., and Khorana, H. G. (2002) Structure and function in rhodopsin: high-level expression of rhodopsin with restricted and homogeneous *N*-

glycosylation by a tetracycline-inducible *N*-acetylglucosaminyltransferase I-negative HEK293S stable mammalian cell line. *Proc. Natl. Acad. Sci. U. S. A.* **99,** 13419–13424

34. Marra, M. N., Wilde, C. G., Griffith, J. E., Snable, J. L., and Scott, R. W. (1990) Bactericidal/permeability-increasing protein has endotoxin-neutralizing activity. *J. Immunol.* **144,** 662–666

35. Hoess, A., Watson, S., Siber, G. R., and Liddington, R. (1993) Crystal structure of an endotoxin-neutralizing protein from the horseshoe crab, *Limulus* anti-LPS factor, at 1.5 Å resolution. *EMBO J.* **12,** 3351–3356

36. Muta, T., Nakamura, T., Hashimoto, R., Morita, T., and Iwanaga, S. (1993) *Limulus* proclotting enzyme. *Methods Enzymol.* **223,** 352–358

37. Hashiguchi, T., Kajikawa, M., Maita, N., Takeda, M., Kuroki, K., Sasaki, K., Kohda, D., Yanagi, Y., and Maenaka, K. (2007) Crystal structure of measles virus hemagglutinin provides insight into effective vaccines. *Proc. Natl. Acad. Sci. U. S. A.* **104,** 19535–19540

38. Aricescu, A. R., Lu, W., and Jones, E. Y. (2006) A time- and cost-efficient system for high-level protein production in mammalian cells. *Acta Crystallogr. D: Biol. Crystallogr.* **62,** 1243–1250

39. Kawabata, S., Miura, T., Morita, T., Kato, H., Fujikawa, K., Iwanaga, S., Takada, K., Kimura, T., and Sakakibara, S. (1988) Highly sensitive peptide-4-methylcoumaryl-7-amide substrates for blood-clotting proteases and trypsin. *Eur. J. Biochem.* **172,** 17–25

40. Mizumura, H., Ogura, N., Aketagawa, J., Aizawa, M., Kobayashi, Y., Kawabata, S., and Oda, T. (2016) Genetic engineering approach to develop next-generation reagents for endotoxin quantification. *Innate Immun.* **23***,* 136–146

41. Segel, I. H. (1975) First-order kinetics. In *Enzyme Kinetics, Behavior and Analysis of Rapid Equilibrium and Steady-state Enzyme Kinetics,* pp. 41–43, John Wiley & Sons, New York

42. Cornish-Bowden, A., and Eisenthal, R. (1978) Estimation of Michaelis constant and maximum velocity from the direct linear plot. *Biochim. Biophys. Acta.* **523,** 268–272

Figure legends

Figure 1. Schematic domain structures of proB and proCE. The two inter-chain disulfide bonds of proB and proCE are indicated by bars, and closed diamonds show *N*-linked glycosylation sites of proB and proCE (13, 14).

Figure 2. The activation of WT proB is quantified by densitometric analysis of Western blotting. *A*, WT proB at varying concentrations from 25 to 200 nM was incubated with WT α-chelicerase C in the presence of LPS at [α-chelicerase C]/[proB] = 1/200 for 30 min at 37°C and subjected to Western blotting with anti-B chain antibody. Data are representative of three independent experiments. *B*, the relative band intensity of the sum total of the WT proB single chain (S), H chain (H), and B chain (B) at each proB concentration to the sum total of the S, H, and B chains at 200 nM proB, as analyzed by ImageJ software. *C*, the rate product formation is shown as the relative band density of the B chain to the total of the S, H, and B chains at each concentration.

Figure 3. The basic residues in the clip domain of proB are required to maintain the activation rate by α-chelicerase C. *A*, WT proB, R17E-proB, K21E-proB, K25E-proB, K38E-proB, or R50E-proB (100 nM) was incubated with WT α-chelicerase C (1.5 nM) in the presence of LPS (60 nM) at 37°C, and aliquots at the indicated times were subjected to Western blotting using anti-B chain antibody. Data are representative of three independent experiments. *B*, the density of the S, H, and B chains was analyzed with Image J software. The *vertical axis* shows the appearance rate of the B chain in each mutant. WT proB (open circles), R17E-proB (closed circles), K21E-proB (open triangles), K25E-proB (closed triangles), K38E-proB (open squares),

R50E-proB (closed squares). *C*, WT-proB (open circles), K21E-proB (open triangles), K25E-proB (closed triangles) or K38E-proB (open squares) (150 nM) was incubated with WT α-chelicerase C (1.0 nM) in the presence of LPS (40 nM), and amidase activities of the resulting WT chelicerase B and the activated mutants at the indicated times were assayed using Boc-L-T-R-MCA. Units of amidase activity were defined as micromoles of the digested synthetic substrate per min, and specific activity was expressed as units per micromole of WT proB or the mutants. Data are the means ± SD of three independent experiments in *B* and *C*. *$P < 0.05$; **$P < 0.01$; ***$P < 0.001$.

Figure 4. The hydrophobic cavity in arthropod clip domains. *A*, sequence alignment of clip domains in arthropods. The basic residues in the clip domain of proB are shown in bold blue letters; the conserved hydrophobic residues at the hydrophobic cavity in *Hd*-PPAF-II, *Dm*-grass, or *Ms*-PAP2 are indicated by dots. The V-55 residue of proB and the V-53 residue of proCE are also indicated by dots; the cysteine resides in the clip domains are indicated by brackets. *B*, the crystal structure of the clip domain of *Hd*-PPAF-II (29) and the basis residues in the clip domain of proB are superimposed. The three dimensional structure (Protein data bank 2B9L) was drawn by CueMol, the free software from Molecular Visualization Framework.

Figure 5. Comparison of the activation rate of V55A-proB with that of WT proB. *A*, WT proB or V55A-proB (100 nM) was incubated with WT α-chelicerase C (1.0 nM) in the presence of LPS (40 nM) at 37°C and aliquots at the indicated times were subjected to Western blotting using anti-B chain antibody. *B*, the density of the S, H, and B chains was analyzed with Image J software. The *vertical axis* shows the appearance rate of the B chain; WT proB (open circles) and V55A-proB (closed circles). *C*, WT proB or V55A-proB (150 nM) was incubated with WT α-

chelicerase C (1.0 nM) in the presence of LPS (40 nM), and amidase activities at the indicated times were assayed using Boc-L-T-R-MCA.; WT proB (open circles) and V55A-proB (closed circles). Units of amidase activity were defined as micromole of the digested synthetic substrate per min, and specific activity was expressed as units per micromole of WT proB or V55A-proB. Data are representative of three independent experiments.in *A*, *B*, and *C*.

Figure 6. Comparison of the activation rate of Δclip-proCE orV53A-proCE with that of WT proCE. *A*, purified WT proCE was subjected to SDS-PAGE and stained with Coomassie Brilliant Blue R-250. An arrowhead indicates WT proCE on SDS-PAGE. *B*, WT proCE, Δclip-proCE or V53A-proCE (50 nM) was incubated with WT chelicerase B (3.0 nM) and LPS (6.0 nM), and aliquots at the indicated times were subjected to Western blotting using anti-H chain antibody. Data are representative of three independent experiments. *C*, the density of the zymogen (S) and the H chain (H) of WT proCE (open circles), Δclip-proCE (closed circles) or V53A-proCE (open triangles) was analyzed with Image J software. The *vertical axis* shows the appearance rate of the H chain. *D,* (50 nM) was incubated with WT chelicerase B (3.0 nM) and LPS (6.0 nM), and amidase activities of WT CE, Δclip-CE or V53A-CE at the indicated times were assayed using Boc-L-G-R-MCA. Units of amidase activity were defined as n mole of the digested synthetic substrate per min, and specific activity was expressed as units per n mole of WT proCE (open circles), Δclip-proCE (closed circles) or V53A-proCE (open triangles). Data are the means ± SD of three independent experiments in *C* and *D*. *$P < 0.05$; **$P < 0.01$; ***$P < 0.001$.

Figure 7. A proposed model for the roles of the clip domains of proB and proCE in the horseshoe crab coagulation cascade. ProC interacts with LPS through the N-terminal tripeptide motif to form oligomers between proC molecules to be transformed to the active transition state

of proC*, leading to autocatalytic conversion to α-chelicerase C. Then, proB is recruited to the reaction center composed of α-chelicerase C and LPS through the clip domain containing the basic residues and the potential hydrophobic cavity to accelerate the formation of ES complex between α-chelicerase C and proB to produce chelicerase B. Finally, the potential hydrophobic cavity in the clip domain of proCE accelerates the formation of another ES complex between chelicerase B and proCE to produce CE.

Tables

Table 1

Kinetic parameters of WT proteases and their mutants in the horseshoe crab coagulation cascade against the peptide substrates.

Proteases	Substrates	K_m (μM)	k_{cat} (s^{-1})	k_{cat}/K_m (M^{-1}s^{-1})
WT α-chelicerase C	Boc-V-P-R-MCA	93 ± 10	34 ± 1	$370,000 \pm 33,000$
WT chelicerase B	Boc-L-T-R-MCA	ND[a)]	ND	$5,300 \pm 57$
K21E-chelicerase B	Boc-L-T-R-MCA	ND	ND	$5,000 \pm 10$
K25E-chelicerase B	Boc-L-T-R-MCA	ND	ND	$4,900 \pm 40$
K38E-chelicerase B	Boc-L-T-R-MCA	ND	ND	$5,100 \pm 47$
V55A-chelicerase B	Boc-L-T-R-MCA	ND	ND	$5,100 \pm 47$
WT CE	Boc-L-G-R-MCA	55 ± 6	194 ± 11	$3,600,000 \pm 410,000$
Δclip-CE	Boc-L-G-R-MCA	47 ± 5	200 ± 9	$4,300,000 \pm 280,000$
V53A-CE	Boc-L-G-R-MCA	46 ± 7	182 ± 3	$4,000,000 \pm 610,000$

Data are the means ± SE of three independent experiments.
[a)] ND, not determined.

Table 2

**Kinetic parameters of WT chelicerase B against two protein substrates.**

Substrates	K_m (nM)	k_{cat} (s^{-1})	k_{cat}/K_m (M^{-1}s^{-1})
WT proCE	190 ± 45	0.04 ± 0.005	$200{,}000 \pm 30{,}000$
V53A-proCE	340 ± 45	0.01 ± 0.001	$30{,}000 \pm 800$

Data are the means $\pm$ SE of three independent experiments.

Prochelicerase B

Proclotting enzyme

Figure 1

Figure 2

Figure 3

A

```
                  17      21    25
ProB (14-37)     CTARG-GLKGSCKSLIDCPSVLATL------
ProCE (11-34)    CSNRF-TEEGTCKNVLDCRILLQKN------
                            •           •
Hd-PPAF-II (58-88)  CGTGADQGKKVCIVYHRCDGVTNTVTPEEVI
                             •               •
Dm-Grass (32-61)    CTTPD-GDQGQCMPFSSCRTIEERLTEAQKA
                             •           •   •
Ms-PAP2 (13-38)     CTLP-NNDKGTCKSLLQCDVASKIISK----
```

```
                          38         50    55
ProB (38-59)     ---------KDSFPVVCSWNGRFQPIVCCPD
ProCE (35-56)    -------DYNLLKESICGF-EGITPKVCCP
                                               •
Hd-PPAF-II (89-116) NTTGEGIFDIRENANECESY----LDVCCGLP
                                               •
Dm-Grass (62-90)    GQKVPADYASYLQKALCGEFNGVR-HFCCP
                             •                 •
Ms-PAP2 (39-66)     -KPRTAQDEKFLRESACGF-QGQTPKVCCP
                            ••
```

B

Figure 4

A

B

C

Figure 5

A

(kDa)
75 —
50 — ◄ WT proCE
37 —
25 —

B

min
0 1 2 5 10 15

(kDa)
75 —
50 —   ◄ S
37 —
                        ◄ H
25 —

WT proCE

min
0 1 2 5 10 15

ΔClip-proCE

min
0 1 2 5 10 15

V53A-proCE

C

Relative band intensity H / (S + H)

Incubation time (min)

D

Activity of CE

Incubation time (min)

Figure 6

Figure 7

Part 2

A mutant equipped with a regenerated disulphide for the missing His loop of a serine protease zymogen in the horseshoe crab coagulation cascade

Abbreviations

AMC, 7-amino-4-methylcoumarin

Boc, *t*-butoxycarbonyl

BSA, bovine serum albumin

CE, clotting enzyme

GnTI, *N*-acetylglucosaminyltransferase I

HLDS, His-loop disulfide

LPS, lipopolysaccharide

MCA, 4-methylcoumaryl-7-amide

MLDS, Met-loop disulfide

PEG-PCMal, polyethylene glycol-photocleavable maleimide

proB, prochelicerase B

proC, prochelicerase C

proCE, proclotting enzyme

proG, prochelicerase G

RCL, reactive center loop

SEC, serpin-enzyme complex

SEM, standard error of the mean

SLDS, Ser-loop disulfide

WT, wild type

Abstract

The lipopolysaccharide-triggered coagulation cascade in horseshoe crabs is composed of three zymogens belonging to the trypsinogen family: prochelicerase C, prochelicerase B (proB), and the proclotting enzyme (proCE). Trypsinogen-family members contain three conserved disulfides located around the active site. While it is known that proB evolutionarily lost one of the disulfides, the His-loop disulfide, the roles of the missing His-loop disulfide in proB remain unknown. Here we prepared a proB mutant, named proB-murasame, equipped with a regenerated His-loop disulfide. The activation rate by upstream α-chelicerase C for proB-murasame was indistinguishable from that for wild-type (WT) proB. The resulting protease chelicerase B-murasame exhibited an 8-fold higher k_{cat} value for downstream proCE than WT chelicerase B, whereas the K_m value of chelicerase B-murasame was equivalent to that of WT chelicerase B. WT serpins-1, -2, and -3, identified as scavengers for the cascade, had no reactivity against WT chelicerase B, whereas chelicerase B-murasame was inhibited by WT serpin-2, suggesting that WT chelicerae B may trigger as-yet-unsolved phenomena after performing its duty in the cascade. The reconstituted lipopolysaccharide-triggered cascade containing proB-murasame exhibited ~5-fold higher CE production than that containing WT proB. ProB-murasame might be used as a high value-adding reagent for lipopolysaccharide detection.

Key words: hemolymph coagulation; lipopolysaccharide; recombinant protein; serine protease; serpin.

Introduction

We recently proposed new terms for three serine protease zymogens that make up the horseshoe crab coagulation cascade—prochelicerase C (proC), prochelicerase B (proB), and prochelicerase G (proG), for factor C, factor B, and factor G, respectively—since the identical or similar terms are used for the protease zymogens in the complement systems in both Chelicerata and Vertebrata (*1*). The horseshoe crab coagulation cascade is triggered by the autocatalytic activation of proC to the active form through an active transition state of proC responding to bacterial lipopolysaccharide (LPS), and the resulting α-chelicerase C activates proB to chelicerase B on the surface of LPS, which activates the proclotting enzyme (proCE) to the clotting enzyme (CE) to convert a clottable protein coagulogen into coagulin (*1-3*).

In the absence of LPS, chymotrypsin artificially converts proC into β-chelicerase C, which contains an additional proteolytic cleavage in the N-terminal Cys-rich domain of proC; compared to α-chelicerase C, β-chelicerase C retains ~70% of the amidase activity against a specific peptide substrate, but β-chelicerase C exhibits neither the LPS-binding activity nor the converting activity for proB because of the destruction of the LPS binding site of proC by the additional chymotryptic cleavage near the LPS-binding site (*4, 5*). On the other hand, the *N*-terminal clip domain of proB, the second LPS-binding protease zymogen, plays an essential role in binding proB to the surface of LPS to initiate effective proteolytic activation by α-chelicerase C (*3*). As an alternative approach, a β-1,3-D-glucan-sensitive protease zymogen proG is autocatalytically activated to chelicerase G, which directly activates proCE to CE without the aid of proB (*2*).

Activated forms of the trypsinogen- or chymotrypsinogen-family members cleave peptide bonds with strikingly different substrate specificities through the identical charge-relay system of the catalytic triad composed of His[57], Asp[102], and Ser[195] in the chymotrypsinogen numbering and three disulfide bridges to form three independent loops that are conserved: the His-loop disulfide (HLDS, Cys[42]–Cys[58]),

the Met-loop disulfide (MLDS, Cys^{168}–Cys^{182}), and the Ser-loop disulfide (SLDS, Cys^{191}–Cys^{220}) (*6, 7*) (Fig. 1A). These disulfide loops are also conserved in proC (*8*), proG (*9*), and proCE (*10*) in the Japanese horseshoe crab *Tachypleus tridentatus*, whereas proB lacks the HLDS due to the substitution of Ala (corresponding to Ala^{170} in proB) for Cys^{58}, and the counterpart Cys^{42} (corresponding to Cys^{154} in proB) is presumed to exist as a free cysteine residue or to form a mixed disulfide linked with cysteine or a small compound such as glutathione (*11*) (Fig. 1B). The missing HLDS is also observed in proB derived from the American horseshoe crab *Limulus polyphemus* by the identical replacement at the corresponding position (Fig. 1B), indicating that an ancestor of proB lost the HLDS before the divergence between the two species at least 130 million years ago (*12, 13*). Therefore, the missing HLDS in proB is evolutionarily conserved to obtain an unknown advantage in the coagulation cascade or other physiological phenomena, followed by hemolymph coagulation.

In this study, to understand the physiological roles of the missing HLDS in proB, a proB mutant equipped with a regenerated HLDS, named proB-murasame, was biochemically characterized. "Murasame" is a legendary Japanese sword. Here we found that chelicerase B-murasame, exhibits an order of magnitude stronger catalytic activity than the wild-type (WT) chelicerase B. On the other hand, a reagent prepared from hemocyte lysates of horseshoe crabs has been used for the "*Limulus test*", a sensitivity test to detect LPS (*14-16*). We propose here an application of proB-murasame as a high value-adding reagent for LPS detection.

Experimental procedures

Materials

HEK293S GnTI⁻ cells were obtained from ATCC. LPS derived from *Salmonella minnesota* R595 (Re) was purchased from List Biological Laboratories, Inc. (Campbell, CA). An average molecular weight of 2,500 for *S. minnesota* R595 (Re) LPS was used for the determination of molecular concentrations.

Cloning and mutagenesis of WT proB, proB-murasame, the R103A-proB mutant and the three serpins-1, -2, and -3

WT proB and WT proCE were subcloned into vector pCA7 as described previously (*3*, *17*, *18*). ProB-murasame and the R103A-proB mutant were constructed by inverse PCR. Full length DNA fragments of serpins-1(19), -2 (20) and -3 (21) derived from *T. tridentatus* were subcloned into vector pCA7, and His-tag and podoplanin PA-tag (*1*) were added the N-terminal end of serpins by site-directed mutagenesis using inverse PCR.

Expression and purification of the recombinant proteins

The recombinant proteins including WT proC (*1*, *4*), WT proB (*3*, *17*), WT proB-murasame, the R103A-proB mutant, WT serpin-1, WT-serpin-2, and WT serpin-3 were expressed in an HEK293S cell line lacking *N*-acetylglucosaminyltransferase I (GnTI⁻). The recombinant proteins in culture media were mixed with 50 mM Na phosphate, pH 8.0, containing 150 mM NaCl and 10 mM imidazole at final concentrations and applied to a Ni-NTA-agarose column (1.0 × 10 cm). The column was washed with the same buffer and the recombinant proteins were eluted with 20 mM Tris-HCl, pH 8.0, containing 150 mM NaCl and 50–200 mM imidazole. The resulting samples were dialyzed against 20 mM Tris-HCl, pH 8.0, containing 150 mM NaCl. The concentrations of the recombinant proteins were determined using a Micro BCA™ protein assay Kit (Thermo Scientific). The purified recombinant proteins used for

this study were analyzed by SDS-PAGE (Supplemental Fig. S1).

Activation of WT proB, the R103A-proB mutant and proB-murasame

WT proC (160 nM) was autocatalytically activated in the presence of 3.2 μM LPS for 30 min at 37ºC. The resulting WT α-chelicerase C was diluted with 20 mM Tris-HCl, pH 8.0, containing 150 mM NaCl and 0.1 mg/ml of bovine serum albumin (BSA). WT proB or proB-murasame (50nM) was activated by WT α-chelicerase C (1 nM) in 20 mM Tris-HCl, pH 8.0, containing 150 mM NaCl and 0.1 mg/ml of BSA at 37ºC. The appearance of the B chain of WT proB, the R103A-proB mutant or proB-murasame was detected by Western blotting.

Measurement of amidase activity of WT chelicerase B and chelicerase B-murasame

WT proC (160 nM) was autocatalytically activated in the presence of 6.4 μM LPS for 30 min at 37ºC. The resulting WT α-chelicerase C was diluted with 20 mM Tris-HCl, pH 8.0, containing 150 mM NaCl and 0.1 mg/ml of BSA. WT proB or proB-murasame (150 nM) was activated by 1.5 nM WT α-chelicerase C in 20 mM Tris-HCl, pH 8.0, containing 150 mM NaCl and 0.1 mg/ml of BSA at 37ºC. The amidase activities of the aliquots at the indicated times were determined by incubation with 0.4 mM *t*-butoxycarbonyl (Boc)-Leu-Thr-Arg-4-methylcoumaryl-7-amide (MCA) (Peptide Institute, Osaka, Japan) for 5 min at 37ºC, and 10% acetic acid was added to terminate the reaction. The rate of substrate hydrolysis was measured fluorometrically with excitation at 380 nm and emission at 440 nm (*22*).

Polyethylene glycol-switch assay

WT proB or proB-murasame (5.0 μM) was incubated with 500 μM polyethylene glycol-photocleavable maleimide (PEG-PCMal) (Dojindo, Kumamoto, Japan) in 50 mM Tris-HCl, pH 7.5, containing 0.1 M NaCl for 90 min at 37ºC under the pH conditions recommended by the reagent protocol. Unreacted PEG-PCMal was removed by methanol/chloroform protein precipitation. The pellet was dissolved in

sampling buffer containing 2-mercaptoethanol. Samples were subjected to SDS-PAGE in 10% slab gel. The gel was irradiated with UV (302 nm) before being transferred to a polyvinylidene difluoride membrane.

Activation of WT proCE

WT proB or proB-murasame (1.0 nM) was converted to the corresponding active enzyme by incubation with 1.7 nM WT α-chelicerase C in 20 mM Tris-HCl, pH 8.0, containing 150 mM NaCl for 15 min at 37ºC. The resulting WT chelicerase B or chelicerase B-murasame (0.5 nM) was incubated with WT proCE (50 nM). The appearance of the H chain of WT proCE was detected by Western blotting.

Measurement of reactivity of WT serpins-1, -2, and -3 against WT chelicerase B and chelicerase B-murasame

WT serpin-1, -2, or -3 (400 nM) was incubated with 80 nM WT chelicerase B or chelicerase B-murasame in 20 mM Tris-HCl, pH 8.0, containing 150 mM NaCl and 0.1 mg/ml of BSA for 30 min at 37ºC. The residual amidase activities of the aliquots were determined by incubation with 0.4 mM Boc-Leu-Thr-Arg-MCA for 5 min at 37ºC. The rate of substrate hydrolysis was measured as described in the subsection entitled *Measurement of amidase activity of WT chelicerase B and chelicerase B-murasame*. The second-order rete constant (k_i) for the inhibition of chelicerase B-murasame by WT serpin-2 was determined as previously described (*19-21*). In brief, chelicerase B-murasame (50 nM) was incubated with WT serpin-2 (150 nM) in 20 mM Tris-HCl, pH 8.0, containing 150 mM NaCl and 0.1 mg/ml of BSA at 37ºC. At appropriate times (5 to 20 min), 10-µl aliquots were removed, and the reaction was terminated by the addition of 90 µl of the buffer containing 0.4 M mM Boc-Leu-Thr-Arg-MCA and the residual activity were determined at 37ºC. The k_i value was calculated using the standard equation for a second order reaction (*23*).

SDS-PAGE and Western blotting

Samples were subjected to SDS-PAGE in 12% slab gel according to the method of Laemmli (*24*). and

the gels were stained Coomassie Brilliant Blue R-250. For Western blotting, gels were transferred to a

polyvinylidene difluoride membrane. After blocking with 5% non-fat dry milk for 30 min, the membrane

was incubated with rabbit polyclonal antibody to the B-chain of chelicerase B (*3*) or the H-chain of CE

(*17*), and then horseradish peroxidase conjugated secondary antibody (Bio Rad Laboratories, Hercules,

CA) was applied. The membranes were then developed with Western Bright Sirius or ECL (Advansta,

Menlo Park, CA). Images were obtained by an Omega Lum G imaging system (Aplegen Life Sciences,

San Francisco, CA).

Kinetic analysis for the reaction between chelicerase B-murasame and Boc-Leu-Thr-Arg-MCA

Chelicerase B-murasame or WT chelicerase B was incubated with Boc-Leu-Thr-Arg-MCA at 37ºC in

20 mM Tris-HCl, pH 8.0, containing 150 mM NaCl and 0.1 mg/ml of BSA. The initial rate of hydrolysis

was measured fluorometrically with excitation at 380 nm and emission at 440 nm after adding the

substrate solution. A kinetic parameter (k_{cat}/K_m) of WT chelicerase B or chelicerase B-murasame was

determined under the condition of [S] < K_m ([S] = 50 μM) at the enzyme concentration of 10 nM, as

previously reported (*17*). When this condition is used, the Michaelis-Menten equation $v = k_{cat}[E]_t[S]$ /

(K_m + [S]) reduces to, since the sum total of K_m + [S] is almost equal to K_m.

Kinetic analysis for the reaction between chelicerase B-murasame and the protein substrate WT
ProCE

Chelicerase B-murasame was incubated with WT proCE at 37ºC in the cuvette of a spectrofluorometer

containing 20 mM Tris-HCl, pH 8.0, 150 mM NaCl, 0.1 mg/ml of BSA, and 0.2 mM Boc-Leu-Gly-Arg-

MCA, the specific peptide substrate for CE (Peptide Institute, Osaka, Japan). The hydrolysis of the

peptide substrate by the resulting WT CE was measured continuously, and the rates of the hydrolysis of

the peptide substrate were calculated by the tangential velocities of the hydrolysis curves. The concentration of WT CE converted from WT proCE by chelicerase B-murasame was calculated using the k_{cat} value of WT CE, as previously described (*17*). Kinetic parameters for the reaction between chelicerase B-murasame and WT proCE were determined by direct liner plotting (*25*), using the protein substrate concentrations of 50 nM, 100 nM, 150 nM, 200 nM, and 300 nM and enzyme concentrations of 0.1 nM or 0.05 nM.

Measurement of thermal stability of chelicerase B-murasame and proB-murasame

ProB-murasame or WT proB (100 nM) was activated by 5 nM WT α-chelicerase C for 60 min at 37ºC in 20 mM Tris-HCl, pH 8.0, containing 150 mM NaCl and 0.1 mg/ml of BSA. To examine thermal stability at 37ºC, the resulting chelicerase B-murasame or WT chelicerase B (100 nM) was incubated at 37°C and aliquots were removed at appropriate times (5 to 60 min) and the residual amidase activity was assayed using 0.4 mM Boc-Leu-Thr-Arg-MCA. Next, chelicerase B-murasame or WT chelicerase B (100 nM) was heat-treated at various temperatures (37–90°C) for 10 min. After cooling on ice, the residual amidase activity of the aliquots was determined by incubation with 0.4 mM Boc-Leu-Thr-Arg-MCA for 5 min at 37ºC.

For measurement of the thermal stability of the zymogens, proB-murasame or WT proB (100 nM) was heat-treated at various temperatures (37–90ºC) for 10 min in 20 mM Tris-HCl, pH 8.0, containing 150 mM NaCl and 0.1 mg/ml of BSA. After cooling on ice, 50 nM of heat-treated WT proB or proB-murasame was activated by incubation with 1.0 nM WT α-chelicerase C for 60 min in the presence of 40 nM LPS. The residual amidase activity of the aliquots was determined by using 0.4 mM Boc-Leu-Thr-Arg-MCA for 5 min at 37ºC. The rate of substrate hydrolysis was measured as described in the subsection entitled *Measurement of amidase activity of WT chelicerase B and chelicerase B-murasame*.

Statistical analysis

Statistical analysis was performed by paired t-tests. P-values < 0.05 were considered to be statistically significant.

Results

Proteolytic activation of WT proB by WT α-chelicerase C requires a proper order of the two-step cleavages

Native proB purified from hemocytes is a mixture of the single-chain and two-chains forms of zymogen, both of which are converted to active chelicerase B by α-chelicerase C in the presence of LPS (*3, 26*). The -Arg^{103}-Ser^{104}- bond of proB (the cleavage site 1) is cleaved to form the two-chain form of zymogen by an unknown protease on the secretion pathway in hemocytes or by α-chelicerase C after secretion, and as a result, the two-chain form of zymogen appears, followed by cleavage at the -Ile^{124}-Ile^{125}- bond (the cleavage site 2) by α-chelicerase C to convert the two-chain form of zymogen to the active two-chain form of chelicerase B (Fig. 1C) (*11*). WT proB, prepared in HEK293S GnTI⁻ cells, also contains the two forms of zymogen, and the activation rate of WT proB is assessed by detecting the appearance of the B chain through the cleavage at site 2 by Western blotting using an anti-B chain antibody (*17*).

To determine whether the two cleavage reactions at the sites 1 and 2 require a proper order to produce the active two-chain form protease of chelicerase B, a non-cleavable mutant at site 1, i.e., a mutant for proB (R103A-proB) in which Arg^{103} is replaced with Ala, was prepared. WT proB and the R103A-proB mutant were respectively incubated with WT α-chelicerase C in the presence of LPS and subjected to Western blotting (Fig. 2A). The B chain of WT chelicerase B appeared at 5 min of incubation and the cleavage reaction at site 2 increased in an incubation time-dependent manner (Fig. 2A, *left panel* and Fig. 2B).

In contrast, the appearance of the B chain derived from the R103A-proB mutant was very slow, compared to the appearance of the B chain derived from WT proB, and a faint band of the B chain was observed by Western blotting after 20 min of incubation (Fig. 2A, *right panel* and Fig. 2B), indicating that the proteolytic conversion of proB to chelicerase B through the two cleavage reactions requires the proper order—namely, the cleavage reaction at site 1 must precede that at site 2.

Preparation of ProB-murasame equipped with a regenerated disulfide for the missing HLDS and confirmation of the HLDS formation in ProB-murasame

To regenerate the missing HLDS in WT proB, Ala[170] in proB was replaced with Cys using site-directed mutagenesis to obtain proB-murasame as described below in the **Experimental procedures**. To determine whether Cys[170] introduced in proB-murasame interacts with Cys[154] to form the HLDS, a polyethylene glycol-switch assay was conducted by using the thiol-binding reagent, PEG-PCMal.

In the PEG-PCMal system, proteins reacted with the reagent result in lower mobility by ~5 kDa per free-Cys residue on SDS-PAGE. WT proB or proB-murasame was incubated with a 100-fold molar excess of PEG-PCMal and subjected to Western blotting using the anti-B chain antibody. PEG-PCMal was incorporated into the single-chain form of WT proB with 55 kDa or the H chain of the two-chain form of WT proB with 35 kDa, resulting in the lower mobility protein bands of 60 kDa and 40 kDa, respectively (Fig. 3, *lanes 1* and *2*). About 60% of the single-chain form of WT proB and the H chain of the two-chain form of WT proB were modified with PEG-PCMal, based on the densitometric analysis, suggesting that ~40% of Cys[154] of WT chelicerase B in this preparation may form a mixed disulfide linked with cysteine or a small compound such as glutathione. In contrast, no band shift was observed in proB-murasame in the presence of PEG-PCMal under the same conditions used for WT proB (Fig. 3, *lanes 3* and *4*). These findings indicate that Cys[170] substituted in proB-murasame reacts with Cys[154] to regenerate the HLDS.

The conversion rate of proB-murasame into chelicerase B-murasame by WT α-chelicerase C

To determine whether the substitution of Ala[170] to Cys affects the activation rate of proB-murasame by WT α-chelicerase C, WT proB and proB-murasame were respectively incubated with WT α-chelicerase C in the presence of LPS and subjected to Western blotting using the anti-B chain of chelicerase B. The conversion rate of proB-murasame into chelicerase B-murasame by α-chelicerase C was

indistinguishable from that of WT proB into WT chelicerase B by α-chelicerase C (Fig. 4A and B), indicating that the Ala[170] to Cys substitution has no effect on the conversion rate of proB-murasame into chelicerase B-murasame by α-chelicerase C.

The activating samples of WT proB and proB-murasame by α-chelicerase C exhibited amidase activity for a specific peptide substrate, Boc-Leu-Thr-Arg-MCA (*17*, *26*), which was correlated with the conversion of WT proB into WT chelicerase B (Fig. 4C). Surprisingly, chelicerase B-murasame exhibited at least an order of magnitude stronger amidase activity than WT chelicerase B (Fig. 4C).

Determination of the kcat/Km value of chelicerase B-murasame for the specific peptide substrate

We previously determined the k_{cat}/K_m value of WT chelicerase B for the Boc-Leu-Thr-Arg-MCA (k_{cat}/K_m = 5,300 M^{-1} s^{-1}), rather than an independent K_m or k_{cat} value for the substrate, because WT chelicerase B showed a very large K_m value (> 200 μM) for the peptide substrate (*17*). In this study, the k_{cat}/K_m value of chelicerase B-murasame for this peptide substrate was determined under conditions identical to those in the previous study, i.e., [S] < K_m at the enzyme concentration of 10 nM, as described in the **Experimental procedures**. ProB-murasame or WT proB was fully converted into the active form by a 6-h incubation at 37ºC with WT α-chelicerase C in the presence of LPS. As expected, the k_{cat}/K_m of the resulting chelicerase B-murasame was much higher than the corresponding value for WT chelicerase B—i.e., chelicerase B-murasame had a k_{cat}/K_m value of 70,000 M^{-1} s^{-1}, 13-fold higher than that of the WT chelicerase B (Table I).

The proteolytic activity of chelicerase B-murasame for the conversion of the protein substrate WT proCE into WT CE

To examine whether chelicerase B-murasame exhibits higher proteolytic activity for the conversion of the protein substrate WT proCE than WT chelicerase B, chelicerase B-murasame and WT chelicerase B were respectively incubated with WT proCE at [E]/[S] = 1/100, and the time course of proteolytic

conversion of proCE to CE was evaluated by the appearance of the H chain of CE on Western blotting using an antibody to the H chain of CE (Fig 5A). The relative band intensity of the H chain of WT CE produced by chelicerase B-murasame at 1-min incubation was 6.5-fold higher than that produced by WT chelicerase B (Fig. 5B), indicating that the proteolytic activity of chelicerase B-murasame for the conversion of WT proCE to CE is higher than that of WT chelicerase B.

Kinetic parameters of chelicerase B-murasame for the protein substrate WT proCE

We previously determined the kinetic parameters of WT chelicerase B for the protein substrate WT proCE (*17*). Using the same kinetic methodology, the kinetic parameters of chelicerase B-murasame for WT proCE were determined as described in the **Experimental procedures**. The K_m value of chelicerase B-murasame was equivalent to that of WT chelicerase B, whereas the k_{cat} value of chelicerase B-murasame was ~8-fold higher than that of WT chelicerase B, resulting in an 8.5-fold higher k_{cat}/K_m value of chelicerase B-murasame compared to that of WT chelicerase B (Table II).

Thermal stability of chelicerase B-murasame and proB-murasame

WT chelicerase B and chelicerase B-murasame maintained their original amidase activity during the incubation at 37ºC for at least 60 min (Fig. 6A). Due to the regeneration of the HLDS in chelicerase B-murasame, we considered that chelicerase B-murasame might retain more structural stability than WT chelicerase B. To examine this possibility, we analyzed the thermal stability of chelicerase B-murasame, chelicerase B-murasame and WT chelicerase B by heat-treating each for 10 min at 37–90ºC, and measuring their remaining amidase activities at 37ºC using Boc-Leu-Thr-Arg-MCA. The amidase activity of WT chelicerase B decreased rapidly after the heat treatment at 50ºC and almost disappeared at 60ºC. In contrast, chelicerase B-murasame maintained ~60% of the original amidase activity after the heat treatment at 60ºC (Fig. 6B).

To examine the thermal stability of their zymogens, proB-murasame and WT proB were also heat-

treated under the identical conditions, and then the heat-treated zymogens were activated by WT α-chelicerase C, and the resulting amidase activities of the converted proteases were assayed. The heat-treatment of WT proB at 50ºC resulted in the complete loss of the original amidase activity, whereas proB-murasame retained ~65% of the original amidase activity after the heat-treatment at 50ºC under the identical conditions (Fig. 6C). These findings indicate that the regeneration of the HLDS reinforced the thermal stability of both chelicerase B-murasame and proB-murasame.

The reactivity of serpins against WT chelicerase B and chelicerase B-murasame

When a serpin-protease complex is formed through the nucleophilic attack of Ser[195] of a target serine protease against the cleavage site on the reactive center loop (RCL) of a serpin to form an ester bond (Fig. 7A), the serpin undergoes its conformational changes at a rate faster than the hydrolysis of the ester bond and twists the three-dimensional arrangement of the catalytic triads of the target protease so that the hydrolysis of the ester bond occurs at an extremely low speed (*27*, *28*).

Three horseshoe crab serpins have been identified from hemocytes, serpin-1 (*19*), serpin-2 (*20*), and serpin-3 (*21*), and each exhibits different selectivity, depending on the sequences of the corresponding cleavage sites at their RCLs (Fig. 7A): serpins-1, -2, and -3 specifically inhibit α-chelicerase C, CE, and chelicerase G, respectively (*19-21*). However, the reactivity of these serpins against chelicerase B has not been examined. To examine this reactivity, we prepared WT serpins-1, -2, and -3 in HEK293S GnTI⁻ cells.

To determine the reactivity of the three serpins against WT chelicerase B and chelicerase B-murasame, each WT serpin was mixed with WT chelicerase B or chelicerase B-murasame; the remaining activity was then measured using Boc-Leu-Thr-Arg-MCA. None of the three WT serpins inhibited the amidase activity of WT chelicerase B at a 5-molar excess of each WT serpin against WT chelicerase B (Fig. 7B). In contrast, the original activity of chelicerase B-murasame was almost inhibited by WT serpin-2 under the identical conditions (Fig.7B). The second-order rate constant for inhibition of

chelicerase B-murasame by WT serpin-2 was determined to be $k_i = 6.0 \times 10^3 \pm 0.7 \times 10^3$ M^{-1}s^{-1}.

Native chelicerase B purified from hemocytes exhibited Arg specificity at the P1 site of synthetic peptide substrates (26) and therefore, there is a possibility that the regenerated HLDS in chelicerase B-murasame may change the substrate specificity at the P1 site of chelicerase B from Arg to Lys, since the cleavage residue of serpin-2 is Lys[350] (Fig. 7A). However, chelicerase B-murasame and WT chelicerase B did not cleave a peptide substrate for plasmin, Boc-Val-Leu-Lys-MCA, under the same assay conditions used for Boc-Leu-Thr-Arg-MCA.

Effects of proB-murasame on the coagulation cascade reconstituted by recombinant zymogens.
To evaluate the effect of proB-murasame on the LPS-triggered coagulation cascade, the cascade was reconstituted by mixing WT proC, WT proB, and WT proCE (WT cascade-111) or WT proC, proB-murasame, and WT proCE (cascade-murasame-111) at an equimolar ratio of 1:1:1. The expression time-course of the amidase activity of WT CE, the final product produced by the proteolytic cascade triggered in the presence of LPS, was monitored using a specific fluorogenic peptide substrate, Boc-Leu-Gly-Arg-MCA. Typical hydrolysis curves for the expression time-course of the amidase activities of WT CE produced in both the cascade systems triggered by 100 nM LPS are shown in Fig. 8A.

The rates of hydrolysis of the peptide substrate were calculated by the tangential velocities of the hydrolysis curve, and the concentrations of WT CE produced were calculated using the k_{cat} value as described in the **Experimental procedures**. The concentrations of WT CE produced after the 2-min incubation trigged by the different concentrations of LPS were determined and are shown in Fig. 8B. The amount of WT CE produced increased with the dose of LPS from 1.0 to 100 nM in a dose-dependent manner. Throughout the range of these LPS concentrations, the amount of WT CE produced in cascade-murasame-111 was ~5-fold higher than that of WT CE produced in WT cascade-111, indicating that cascade-murasame-111 converted proCE to CE more efficiently than WT cascade-111.

On the other hand, the higher concentrations of LPS (> 100 nM) suppressed the production of WT

CE both in WT cascade-111 and cascade-murasame-111 (Fig. 8B), which phenomenon was also observed in the case of the LPS-triggered autocatalytic activation of native proC isolated form hemocytes (*29*). To extend the linearity of the LPS-dependent production of WT CE in cascade-murasame-111, the cascade was reconstituted by mixing WT proC, proB-murasame, and WT proCE at a molar ratio of 5:1:1 (cascade-murasame-511). As expected, the linearity of the LPS dose-dependency in cascade-murasame-511 was expanded, ranging from 1.0 to 1,000 nM (Fig. 8C).

Discussion

The three independent disulfides, HLDS, MLDS, and SLDS, are conserved in the trypsinogen- or chymotrypsinogen-family members and are located around the catalytic triad and the substrate binding pocket (Fig. 1A). Each of them may contribute to stabilization of the tertiary structure of these family members, leading to the retention of the catalytic activity. However, proB, one of the zymogens constituting the LPS-triggered horseshoe crab coagulation cascade, evolutionarily lost the HLDS. Moreover, several serine protease zymogens involved in the mammalian complement system, including C1r (*30*, *31*), C1s (*32*), and MASP2 (*33*), also evolutionarily lost their HLDS (Fig. 1B). Sim reported that the substrate specificity of the activated C1r for synthetic ester substrates is very narrow, whereas that of the activated C1s is broad, allowing C1s to hydrolyze a wide range of ester substrates (*34*). Therefore, Arlaud and Gagnon demonstrated that the missing HLDS in C1r and C1s cannot be related to precise functional characteristics of C1r or C1s; though both complement factors differ from most other mammalian serine proteases *in vivo*, they function in a high-molecular weight complex, not as dissociated enzymes (*35*).

In this study, a recombinant with the HLDS regenerated in proB, named proB-murasame, was prepared. ProB-murasame was converted into the active form chelicerase B-murasame by WT α-chelicerase C in the presence of LPS at a conversion rate indistinguishable from that of WT proB (Fig. 4, A and B). The regeneration of the HLDS caused the k_{cat}/K_m value of chelicerase B-murasame for the specific peptide substrate to be 13-fold higher than that of WT chelicerase B (Table I). For the protein substrate WT proCE, chelicerase B-murasame exhibited an 8-fold higher k_{cat} value than that of WT chelicerase B, whereas the K_m value of chelicerase B-murasame was equivalent to that of WT chelicerase B (Table II). These findings suggest that HLDS contributes to the maintenance of an optimal three-dimensional conformation around the catalytic triad to increase the catalytic turnover number of chelicerase B-murasame.

Previously, Varallyay *et al*. found that elimination of the SLDS in chymotrypsin or trypsin by the replacement of Cys[191] with Ala using site direct mutagenesis caused a decrease in the k_{cat}/K_m values of two to three orders of magnitude to their specific peptide substrates, mainly as a consequence of an increase in the K_m values, indicating that the SLDS in chymotrypsin or trypsin family members is essential to maintain their substrate recognition (*36*). On the other hand, the effect of the missing HLDS on the catalytic activity of chelicerase B may become clear, when the k_{cat}/K_m value of chelicerase B is compared with that of CE, which is equipped with the HLDS in the identical domain composition to chelicerase B (Fig. 1C); the k_{cat}/K_m value of WT chelicerase B (5,300 M^{-1} s^{-1}) for the specific substrate Boc-Leu-Thr-Arg-MCA is only one seven-hundredth of that of WT CE (3,600,000 M-1 s-1) for the specific substrate Boc-Leu-Gly-Arg-MCA (*17*).

The higher structural stability of chelicerase B-murasame or proB-murasame compared to WT chelicerase B or WT proB was found by comparing their thermal stability (Fig. 6 B and C). Notably, chelicerase B-murasame retained ~60% of its original amidase activity after the heat treatment at 60ºC, although the amidase activity of WT chelicerase B almost disappeared by the heat treatment at 60ºC (Fig. 6 B). These findings indicate that the absence of the HLDS lowers the structural stability of both proB and chelicerase B.

Serpins-1, -2, and -3 are secreted from hemocytes through LPS-induced exocytosis, accompanied by secretion of the coagulation factors proC, proB, proCE, and proG (*2*). Generally, each mammalian serpin functions as a scavenger for a target serine protease that has fulfilled its duty, and the resulting serpin-enzyme complex (SEC) is rapidly cleared from the reaction site through a cell-surface receptor, the SEC receptor, that recognizes a neodomain composed of five hydrophobic amino acid residues exposed on the serpin molecule of the SEC (*28, 37*). The hydrophobic consensus sequence is conserved in the COOH-terminal region of mammalian serpins, and horseshoe crab serpins-1, -2, and -3 also contain a homologous consensus sequence in the corresponding region, indicating the presence of a similar SEC-dependent clearance system in the hemolymph coagulation system in horseshoe crabs (*19-*

Serpins-1, -2 and -3 purified form hemocytes specifically inhibit α-chelicerase C (the second-order rate constant $k_i = 2.5 \times 10^6 \, M^{-1} \, s^{-1}$), CE ($4.3 \times 10^5 \, M^{-1} \, s^{-1}$), and chelicerase G ($3.9 \times 10^5 \, M^{-1} \, s^{-1}$), respectively (*19-21*). The amino acid residue of the reactive site of serpins, corresponding to theP1 site of substrates, generally reflects the substrate specificity of target serine proteases. The cleavage site of serpin-2 is Lys[350] (Fig. 7A) and the selectivity of serpin-2 against target proteases seems to be in good agreement with the previous kinetic study, because serpin-2 strongly inhibits plasmin with Lys specificity at the P1 site ($1.2 \times 10^6 \, M^{-1} s^{-1}$). On the other hand, serpin-2 inhibits CE (described above), human α-thrombin ($2.1 \times 10^5 \, M^{-1} s^{-1}$), and rat salivary kallikrein ($1.4 \times 10^5 \, M^{-1} s^{-1}$) with Arg specificity at the P1 site (*20*). In this study, chelicerase B-murasame but not WT chelicerase B was inhibited by WT serpin-2 with $k_i = 6.0 \times 10^3 \, M^{-1} s^{-1}$. Moreover, chelicerase B-murasame did not cleaved Boc-Val-Leu-Lys-MCA. These findings suggest that serpin-2 has broad selectivity against trypsin-family members with Arg or Lys specificity at the P1 site and that the regeneration of HLDS in chelicerase B does not change its substrate specificity at the P1 site from Arg to Lys.

Interestingly, none of the three WT serpins-1. -2, and -3 exhibited any reactivity to WT chelicerase B (Fig. 7B). These findings suggest that WT chelicerase B escapes from the clearance system through the SEC receptor after performing its duty for the hemolymph coagulation cascade at injured sites, and that the remaining activity of WT chelicerase B on the surface of LPS may play important roles to trigger as-yet-unsolved phenomena in horseshoe crabs, such as clot-clearance, wound healing and restoration of cuticles (Fig. 9).

A reagent prepared from hemocyte lysates of horseshoe crabs is used in the *Limulus* test, a sensitivity test for monitoring LPS contamination in parenteral drugs and biologics. We recently developed an LPS-detection reagent using the recombinants WT proC, WT proB and WT proCE to emerge from our dependence on the limited natural resource of horseshoe crab hemocytes (*16*). Here we showed that cascade-murasame-111 exhibited ~5-fold higher CE production than WT cascade-111

(Fig. 8A and B). In addition, the linearity of the LPS dose-dependency in cascade-murasame-111 could be expanded by increasing the molar ratio of WT proC to the other zymogens, such as cascade-murasame-511 (Fig. 8C), although more detailed experiments are required to obtain optimal conditions for practical use. We propose that proB-murasame might be used as a next-generation reagent for LPS detection, when used together with the high value-adding protease zymogen.

Reference

1. Shibata, T., Kobayashi, Y., Ikeda, Y., and Kawabata, S. (2018) Intermolecular autocatalytic activation of serine protease zymogen factor C through an active transition state responding to lipopolysaccharide. *J. Biol. Chem.* **293**, 11589–11599

2. Kawabata, S. and Muta, T. (2010) Sadaaki Iwanaga: discovery of the lipopolysaccharide- and β-1,3-D-glucan-mediated proteolytic cascade and unique proteins in invertebrate immunity. *J. Biochem.* **147**, 611–618

3. Kobayashi, Y., Takahashi, T., Shibata, T., Ikeda, S., Koshiba, T., Mizumura, H., Oda, T., and Kawabata, S. (2015) Factor B is the second lipopolysaccharide-binding protease zymogen in the horseshoe crab coagulation cascade. *J. Biol. Chem.* **290**, 19379–19386

4. Kobayashi, Y., Shiga, T., Shibata, T., Sako, M., Maenaka, K., Koshiba, T., Mizumura, H., Oda, T., and Kawabata, S. (2014) The N-terminal Arg residue is essential for autocatalytic activation of a lipopolysaccharide-responsive protease zymogen. *J. Biol. Chem.* **289**, 25987–25995

5. Koshiba, T., Hashii, T., and Kawabata, S. (2007) A structural perspective on the interaction between lipopolysaccharide and factor C, a receptor involved in recognition of gram-negative bacteria. *J. Biol. Chem.* **282**, 3962–3967

6. Hartley, B. S. (1970) Homologies in serine proteinase. *Phil. Trans. Roy. Soc. Lond.* B **257**, 77–87

7. Mihalyi, E. (1978) Proteolytic enzymes. In Application of Proteolytic Enzymes to Protein Structure Studies, 2nd Edition, pp. 43–127, CRC Press, Inc., West Palm Beach, FL.

8. Muta, T., Miyata, T., Misumi, Y., Tokunaga, F., Nakamura, T., Toh, Y., Ikehara, Y., and Iwanaga, S. (1991) *Limulus* factor C. An endotoxin-sensitive serine protease zymogen with a mosaic structure of complement-like, epidermal growth factor-like, and lectin-like domains. *J. Biol. Chem.* **266**, 6554–6561

9. Seki, N., Muta, T., Oda, T., Iwaki, D., Kuma, K., Miyata, T., and Iwanaga, S. (1994) Horseshoe crab

(1,3)-β-D-glucan-sensitive coagulation factor G. *J. Biol. Chem.* **269**, 1370–1374

10. Muta, T., Hashimoto, R., Miyata, T., Nishimura, H., Toh, Y., and Iwanaga, S. (1990) Proclotting enzyme from horseshoe crab hemocytes. cDNA cloning, disulfide locations, and subcellular localization. *J. Biol. Chem.* **265**, 22426–22433

11. Muta, T., Oda, T., and Iwanaga, S. (1993) Horseshoe crab coagulation factor B. A unique serine protease zymogen activated by cleavage of an Ile-Ile bond. *J. Biol. Chem.* **268**, 21384–21388

12. Srimal S., Miyata, T., Kawabata, S., Miyata, T., and Iwanaga, S. (1985) The complete amino acid sequence of coagulogen isolated from Southeast Asian horseshoe crab, *Carcinoscorpius rotundicauda. J. Biochem.* **98**, 305–318

13. Zhou, Y., Liang, Y., Yan, Q., Zhang, L., Chen, D., Ruan, L., Kong, Y., Shi, H., Chen, M., and Chen, J. (2020) The draft genome of horseshoe crab *Tachypleus tridentatus* reveals its evolutionary scenario and well-developed innate immunity. *BMC Genomics* **21**, 137–151

14. Levin, J., Hochstein, H. D., and Novitsky, T., J. (2003) Clotting cells and Limulus amebocyte lysate: an amazing analytical tool. In *The American Horseshoe Crab* (Shusetr, C. N., Barlow, R. B., and Brockmann, H. J., eds) pp. 310–340, Harvard University Press, Cambridge, MA

15. Armstrong, P. B. (2003) Internal defense against pathogenic invasion: the immune system. In *The American Horseshoe Crab* (Shusetr, C. N., Barlow, R. B., and Brockmann, H. J., eds) pp. 288–309, Harvard University Press, Cambridge, MA

16. Mizumura, H., Ogura, N., Aketagawa, J., Aizawa, M., Kobayashi, Y., Kawabata, S., and Oda, T. (2017) Genetic engineering approach to develop next-generation reagents for endotoxin quantification. *Innate Immun.* **23**, 136–146

17. Yamashita, K., Shibata, T., Takahashi, T., Kobayashi, Y., and Kawabata, S. (2020) Roles of the clip domains of two protease zymogens in the coagulation cascade in horseshoe crabs. *J. Biol. Chem.* **295**, 8857–8866

18. Hashiguchi, T., Kajikawa, M., Maita, N., Takeda, M., Kuroki, K., Sasaki, K., Kohda, D., Yanagi, Y.,

and Maenaka, K. (2007) Crystal structure of measles virus hemagglutinin provides insight into effective vaccines. *Proc. Natl. Acad. Sci. U. S. A.* **104**, 19535–19540

19. Miura Y., Kawabata, S., and Iwanaga, S. (1994) A *Limulus* intercellular coagulation inhibitor with characteristics of the serpin superfamily. Purification, characterization, and cDNA cloning. *J. Biol. Chem.* **269**, 542–547

20. Miura Y., Kawabata, S., Wakamiya, Y., Nakamura, T., and Iwanaga, S. (1995) A *Limulus* intercellular coagulation inhibitor type 2. Purification, characterization, cDNA cloning, and tissue localization. *J. Biol. Chem.* **270**, 558–565

21. Lal Agarwala, K., Kawabata, S., Miura, Y., Kuroki, Y., and Iwanaga, S. (1996) *Limulus* intracellular coagulation inhibitor type 3. Purification, characterization, cDNA cloning, and tissue localization. *J. Biol. Chem.* **271**, 23768–23774

22. Kawabata, S., Miura, T., Morita, T., Kato, H., Fujikawa, K., Iwanaga, S., Takada, K., Kimura, T., and Sakakibara, S. (1988) Highly sensitive peptide-4-methylcoumaryl-7-amide substrates for blood-clotting proteases and trypsin. *Eur. J. Biochem.* **172**, 17–25

23. Ehrlich, H. J., Gebbink, R. K., Keijer, J., Linders, M., Preissner, K. T., and Pannekoek, H. (1990) Alteration of serpin specificity by a protein cofactor. Vitronection endows plasminogen activator inhibitor 1 with thrombin inhibitory. *J. Biol. Chem*. **265**, 13029-13035

24. Laemmli, U. K. (1970) Cleavage of structure proteins during the assembly of the head of bacteriophage T4. *Nature* **227**, 680-685

25. Cornish-Bowden, A. and Eisenthal, R. (1978) Estimation of Michaelis constant and maximum velocity from the direct linear plot. *Biochim. Biophys. Acta.* **523**, 268–272

26. Nakamura, T., Horiuchi, T., Morita, T., and Iwanaga, T. (1986) Purification and properties of intercellular clotting factor, factor B, from horseshoe crab (*Tachypleus tridentatus*) hemocytes. *J. Biochem*. **99**, 847–857

27. Silverman, G. A., Bird, P. I., Carrell, R. W., Church F. C., Coughlin P. B., Gettins, P. G. W., Irving,

67

J. A., Lomas, D. A., Luke, C. J., Moyer, R. W., Pemberton, P. A., Remold-O'Donnell, E., Salvesen, G. S., Travis, J., and Whisstock, J. C. (2001) The serpins are an expanding superfamily of structurally similar but functionally diverse proteins. Evolution, mechanism of inhibition, novel functions, and a revised nomenclature. *J. Biol. Chem.* **276**, 33293–33296

28. Gettins, P. G. W. and Olson, S. T. (2016) Inhibitory serpins. New insights into their folding, polymerization, regulation and clearance. *Biochem. J.* **473**, 2273–2293

29. Nakamura, T., Tokunaga, F., Morita, T., Iwanaga, S., Kusumoto, S., Shiba, T., Kobayashi, T., and Inoue, K. (1988) Intracellular serine-protease zymogen, factor C, from horseshoe crab hemocytes. Its activation by synthetic lipid A analogues and acidic phospholipids. *Eur. J. Biochem.* **176**, 89–94

30. Leytus, S. P., Kurachi, K., Sakariassen, K. S., and Davie, E. W. (1986) Nucleotide sequence of the cDNA coding for human complement C1r. *Biochemistry* **25**, 4855–4863

31. Journet, A. and Tosi, M. (1986) Cloning and sequencing of full-length cDNA encoding the precursor of human complement C1r. *Biochem. J.* **240**, 783–787

32. Mackinnon, C. M., Carter, P. E., Smyth, S. J., Dunbar, B., and Fothergill J. E. (1987) Molecular cloning of cDNA for human complement component C1s. The complete amino acid sequence. *Eur. J. Biochem.* **169**, 547–553

33. Endo, Y., Takahashi, M., Nakao, M., Saiga, H., Sekine, H., Matsushita, M., Nonaka, M., and Fujita, T. (1998) Two lineage of mannose-binding lectin-associated serine protease (MASP) in vertebrates. *J. Immunol.* **161**, 4924–4930

34. Sim, R. B. (1981) The human complement system serine proteases C1r and C1s and their proenzymes. *Methods Enzymol.* **80**, 26–42

35. Arlaud, G. J. and Gagnon, J. (1981) C1r and C1s subcomponents human complement: two serine proteinases lacking the histidine-loop disulphide bridge. *Bioscience Rep.* **1**, 779–784

36. Varallyay, E., Lengyel Z., Graf, L., and Szilagyi, L. (1997) The role of disulfide bond C191–C220 in trypsin and chymotrypsin. *Biochem. Biophys. Res. Commun.* **230**, 592–596

37. Joslin, G., Fallon, R. J., Bullock, J., Adams, S. P., and Perlmutter, D. H. (1991) The SEC receptor

recognizes a pentapeptide neodomain of -antitrypsin-protease complexes. *J. Biol. Chem.* **266**, 11282–

11288

Figure legends

Fig. 1. The location of the three disulfide bridges around the active site in trypsin, the sequence alignment of the HLDS of serine proteases, and the schematic domain structures of proB and proCE. (**A**) The location of the three disulfide bridges, HLDS, MLDS, and SLDS, is indicated by arrows and dashed circles in the three-dimensional structure of bovine trypsinogen (PDB:1TGB), drawn by PyMOL (Schrödinger) (**B**) The sequence alignment of the HLDS of the horseshoe crab coagulation factors *Tt*-proB (*11*), *Lp*-proB (accession No. XP_013784210), *Tt*-proC (*8*), *Tt*-proCE (*10*), and *Tt*-proG β-subunit (*9*) and the other serine proteases *Hs*-C1r (*30, 31*), *Hs*-C1s (*32*), *Hs*-MASP1 (*33*), *Hs*-MASP2 (*33*), *Bt*-trypsinogen (*6*), and *Bt*-chymotrypsinogen (*6*). *Tt*, *Tachypleus tridentatus*; *Lp*, *Limulus polyphemus*; *Hs*, *Homo sapiens*; *Bt*, *Bos taurus*. The cysteine residues evolutionarily replaced by other amino acids are shown in *bold* letters (**C**) The schematic domain structures of *Tt*-proB (*11*) and *Tt*-proCE (*10*). The three conserved disulfide bridges and the inter-chain disulfide linkages are indicated by *brackets*. The missing HLDS in *Tt*-proB is shown in *gray* bars.

Fig. 2. The proper order of the two-step cleavage reactions is essential for the proteolytic activation of proB by α-chelicerase C. (**A**) WT proB or the R103A-proB mutant (50 nM) was incubated with WT α-chelicerase C (1 nM) in the presence of 20 nM LPS at 37ºC, and aliquots at the incubated times were subjected to Western blotting using the anti-B chains antibody. S, the single chain of WT proB or the R103A-proB mutant; H, the heavy chain of WT proB; B, the B chain derived from WT chelicerase B or the activated R103A-proB mutant. (**B**) The densities of the S, H and B chains derived from WT proB (*open circles*) or the R103A-proB mutant (*closed circles*) were analyzed with ImageJ software, and the relative band intensities of B/(S+H+B) are shown on the *vertical axis*. Data are the means ± SEM of three independent experiments. *$P < 0.05$, **$P < 0.01$, ***$P < 0.001$.

Fig. 3. Disappearance of the reactivity of PEG-PCMal to proB-murasame. WT proB or proB-murasame (5.0 μM) was incubated with PEG-PCMal (500 μM) for 30 min at 37ºC, and aliquots were subjected to Western blotting using anti-B chain antibody. Data are representative of three independent experiments. S, the single chain of WT proB or proB-murasame; H, the heavy chain of WT proB or proB-murasame; S*, the single chain of WT proB modified with PEG-PCMal; H*, the heavy chain of WT proB modified with PEG-PCMal.

Fig. 4. The regenerated HLDS in proB-murasame does not affect the activation rate by WT α-chelicerase C and increases the amidase activity against Boc-Leu-Thr-Arg-MCA. (**A**) WT proB or proB-murasame (50 nM) was incubated with WT α-chelicerase C (5 nM) in the presence of LPS (4 nM) at 37ºC, and aliquots at the incubated times were subjected to Western blotting using anti-B chain antibody. Data are representative of three independent experiments. (**B**) The densities of the single chain of WT proB or proB-murasame (S) and the H (H) and B (B) chains of WT proB (*open circles*) or proB-murasame (*closed circles*) were analyzed with ImageJ software, and the relative band intensities of B/(S+H+B) are shown on the *vertical axis*. *C*, WT proB (*open circles*) or proB-murasame (*closed circles*) (150 nM) was incubated with WT α-chelicerase C (1.5 nM) in the presence of LPS (60 nM), and the amidase activities of the resulting WT chelicerase B and chelicerase B-murasame at the indicated times were assayed using Boc-Leu-Thr-Arg-MCA. Units of amidase activity were defined as micromoles of digested synthetic substrate per min, and specific activity was expressed as units per nanomole of WT proB or proB-murasame. Data are the means ± SEM of three independent experiments. *$P < 0.05$, **$P < 0.01$.

Fig. 5. Chelicerase B-murasame possesses higher proteolytic activity for the conversion of proCE into CE than does WT chelicerase B. (**A**) WT proCE (50 nM) was incubated with WT chelicerase B or chelicerase B-murasame (0.5 nM), and aliquots at the indicated times were subjected to Western

blotting using the anti-H chain (CE) antibody. (**B**) The densities of the single (S) and H (H) chains derived from WT proCE activated by WT chelicerase B (*open circles*) or chelicerase B-murasame (*closed circles*) were analyzed with ImageJ software, and the relative band intensities of H/(S+H) are shown on the *vertical axis*. Data are the means ± SEM of three independent experiments. *$P < 0.05$, **$P < 0.01$, ***$P < 0.001$.

Fig. 6. Thermal stability of WT chelicerase B, chelicerase B-murasame, and their zymogens. (A) WT chelicerase B (*open circles*) or chelicerase B-murasame (*closed circles*) (100 nM) was incubated at 37°C and aliquots were removed at appropriate times (5 to 60 min) and the residual amidase activity was assayed using Boc-Leu-Thr-Arg-MCA. (**B**) WT chelicerase B (*open circles*) or chelicerase B-murasame (*closed circles*) (100 nM) was heat-treated at the indicated temperatures for 10 min. After cooling on ice, the residual amidase activity was assayed using Boc-Leu-Thr-Arg-MCA. (**C**) WT proB (*open circles*) or proB-murasame (*closed circles*) (100 nM) was heat-treated at the indicated temperatures for 10 min. After cooling on ice, the heat-treated zymogens were activated by chelicerase C in the presence of LPS and the residual amidase activities were assayed as described in the **Experimental procedures**. The amidase activities derived from the zymogens incubated at 37°C were defined as 100% activity. Data are the means ± SEM of three independent experiments. *$P < 0.05$, **$P < 0.01$.

Fig. 7. The residual amidase activities of WT chelicerase B and chelicerase B-murasame after the reaction with WT serpins-1, -2, and -3. (A) Three-dimensional structure of human antitrypsin (PDB:1QLP), drawn by PyMOL and putative positions of cleavage sites of horseshoe crab serpins-1, -2, and -3 are shown. The RCL of human antitrypsin is indicated by a dashed ellipse and the estimated position of the reactive site for serpins-1, -2, or -3 is indicated by an arrow. (**B**) Each serpin (400 nM) was incubated with WT chelicerase B or chelicerase B-murasame (80 nM) for 30 min at 37°C, and the

residual amidase activities were assayed using Boc-Leu-Thr-Arg-MCA. Data are the means ± SEM of three independent experiments. **$P < 0.01$.

Fig. 8. Effect of proB-murasame on the coagulation cascade reconstituted by recombinant zymogens. (**A**) A mixture of 10 nM each of WT proC, WT proB, and WT proCE (WT casdade-111, dashed line) or a mixture of 10 nM each of WT proC, proB-murasame, and WT proCE (cascade-murasame-111, solid line) was incubated at 37°C in a cuvette. The proteolytic cascades were triggered by adding 100 nM LPS, and the concentration of 7-amino-4-methylcoumarin (AMC) released from Boc-Leu-Gly-Arg-MCA by the resulting CE was monitored. Data are representative of three independent experiments. (**B**) The mixture of WT cascade-111 (*open circles*) or cascade-murasame-111 (*closed circles*) was incubated at 37°C in a cuvette. The proteolytic cascades were triggered by adding 1-10,000 nM LPS and the concentration of the resulting WT CE per min was estimated from the concentration of AMC at 2-min after adding LPS. Data are the means ± SEM of three independent experiments. (**C**) The mixture of cascade-murasame-111 (*open circles*) or cascade-murasame-511 (50 nM WT proC, 10 nM proB-murasame and 10 nM WT proCE, *closed circles*) was incubated at 37°C in a cuvette. The proteolytic cascades were triggered by adding 1-10,000 nM LPS, and the concentration of the resulting WT CE per min was estimated from the concentration of AMC at 2-min after adding LPS. Data are representative of three independent experiments. *$P < 0.05$, **$P < 0.01$.

Fig. 9. An activation and regulation model for the LPS-triggered hemolymph coagulation in horseshoe crabs. ProC is autocatalytically activated to α-chelicerase C (*shown as the capital letter C*) through an active transition state of proC responding to LPS, and the resulting α-chelicerase C activates proB to chelicerase B (*capital letter B*) on the surface of LPS, which activates proCE to CE (*capital letter CE*). After performing their duties for the cascade, the activated proteases α-chelicerase C and CE, but not chelicerase B, are cleared by reacting with the corresponding scavengers, serpins-1 and -2,

73

respectively, through the SEC receptor system. The remaining activity of chelicerase B on LPS may trigger as-yet-unsolved phenomena, such as clot-clearance, wound healing and restoration of cuticles. The reactive sites of serpins-1 and -2 are indicated by *gray circles* and *gray triangles*, respectively, on their RCLs in gray.

A legend to supplemental figure

Fig. S1. SDS-PAGE analysis of the recombinant proteins used for this study. The recombinant proteins including WT proC, WT proB, proB-murasame, the R103A-proB mutant, WT proCE, WT serpin-1, WT serpin-2, and WT serpin-3 were subjected to SDS-PAGE and stained with Coomassie Brilliant Blue R-250. The letters, S, H, and L, indicate the single chain, the heavy chain, and the light chain of each recombinant protein, respectively. The 18-kDa band of the L chain for the two chain form of WT proB or proB-murasame was not detectable on SDS-PAGE under the conditions used.

Tables

Table I. The k_{cat}/K_m values of chelicerase B-murasame and WT chelicerase B for Boc-Leu-Thr-Arg-MCA[a].

Proteases	k_{cat}/K_m (M^{-1} s^{-1})
Chelicerase B-murasame	$70,000 \pm 2,000$
WT chelicerase B	$5,400 \pm 180$

[a]Data are means ± SEM from three independent experiments.

Table II. The kinetic parameters of chelicerase B-murasame and WT chelicerase B for WT proCE[a].

Proteases	K_m (nM)	k_{cat} (s^{-1})	k_{cat}/K_m (M^{-1} s^{-1})
Chelicerase B-murasame	190 ± 13	0.33 ± 0.08	$1,700,000 \pm 400,000$
WT chelicerase B[b]	190 ± 45	0.04 ± 0.005	$200,000 \pm 30,000$

[a]Data are means $\pm$ SEM from three independent experiments.

[b]These parameters are cited from the ref.17.

Figure 1

Figure 2

Figure 3

Figure 4

A

WT chelicerase B
┌─── min ───┐
(kDa) 0 1 2 5 10 15

75 —

50 — ◄ S
37 —

       ◄ H

25 —

B-murasame
┌─── min ───┐
0 1 2 5 10 15

       ◄ S

       ◄ H

└──────── WT proCE ────────┘

B

Figure 5

Figure 6

A

Reactive sites

Serpin-1(357-360) -G-V-R-S-
Serpin-2(348-351) -M-L-K-S-
Serpin-3(357-360) -G-W-R-S-

B

Figure 7

Figure 8

Figure 9

Supplemental Figure S1

Part 3

Effects of Ca^{2+} ions on the horseshoe crab coagulation cascade triggered by lipopolysaccharide

Abbreviations

AMC, 7-amino-4-methylcoumarin

Boc, *t*-butoxycarbonyl;

CBB, Coomassie Brilliant Blue

CE, clotting enzyme

EDTA, ethylenediaminetetraacetic acid

GnTI, *N*-acetylglucosaminyltransferase I

HEPES, 4-(2-hydroxyethyl)-1-piperazineethanesulfonic acid

HSA, human serum albumin

ITC, isothermal titration calorimetry

LPS, lipopolysaccharide

MCA, 4-methylcoumaryl-7-amide

proB, prochelicerase B

proC, prochelicerase C

proCE, proclotting enzyme

proG, prochelicerase G

SDS-PAGE, sodium dodecyl sulphate-polyacrylamide gel electrophoresis

SEM, standard error of the mean

WT, wild-type.

Abstract

The lipopolysaccharide (LPS)-triggered horseshoe crab coagulation cascade is composed of three protease zymogens, prochelicerase C (proC), prochelicerase B (proB), and the proclotting enzyme (proCE). In this study, we found that Ca^{2+} ions increase the production of the clotting enzyme as a result of a cascade reaction reconstituted by recombinant proteins of wild-type (WT) proC, WT proB, and WT proCE. We divided the cascade into three stages: autocatalytic activation of WT proC on the surface of LPS into WT α-chelicerase C (Stage 1); activation of WT proB on the surface of LPS into WT chelicerase B by WT α-chelicerase C (Stage 2); and activation of WT proCE into WT CE by chelicerase B (Stage 3). Ca^{2+} ions enhanced the proteolytic activation in Stage 2, but not those in Stages 1 and 3. Moreover, we performed isothermal titration calorimetry to clarify the interaction of LPS or the recombinant zymogens with Ca^{2+} ions. LPS interacted with Ca^{2+} ions at an association constant of $K_a = 4.7 \times 10^4 \ M^{-1}$, but not with any of the recombinant zymogens. We concluded that LPS bound with Ca^{2+} ions facilitates the chain reaction of the cascade as a more efficient scaffold than LPS itself.

Key words: horseshoe crab hemolymph coagulation; lipopolysaccharide; recombinant protein; serine protease; calcium ions

Introduction

The horseshoe crab hemolymph coagulation cascade consists of four serine protease zymogens—prochelicerase C (proC), prochelicerase B (proB), prochelicerase G (proG), and the proclotting enzyme (proCE) —and the clottable protein coagulogen (Fig. 1A) (1,2). The two branched initial activation steps in the cascade consist of autocatalytic activation of proC upon its binding to lipopolysaccharide (LPS) derived from Gram-negative negative bacteria, and autocatalytic activation of proG upon its binding to β-1, 3-D-glucan derived from fungi or algae. ProC interacts with LPS with a dissociation constant of K_d = 7.56×10^{-10} M *via* an N-terminal LPS-binding site composed of Arg[36]-Trp[37]-Arg[38] to form an oligomer on LPS (Fig. 1B) (3, 4) and is autocatalytically activated into α-chelicerase C through an active transition state of proC (5). α-Chelicerase C activates proB into chelicerase B on the surface of LPS. Notably, there are two cleavage sites in proB, the Arg[104]-Ser[105] (site 1) and Ile[124]-Ile[125] bonds (site 2) (Fig. 1B), and depending on the lot in which proB is prepared, the two-chain-form zymogen (the H and L chains) of proB cleaved at the site 1 may be present in the preparation (6). We found recently that the proteolytic conversion of proB to chelicerase B through the two cleavage reactions requires the proper order—namely, the cleavage reaction at site 1 must precede that at site 2 (7). The resulting chelicerase B activates proCE into the clotting enzyme (CE) that converts coagulogen to coagulin, leading to the formation of insoluble coagulin gel by its head-to-tail polymerization (8). On the other hand, proG on β-1, 3-D-glucan is autocatalytically activated into chelicerase G, which directly converts proCE to CE without the aid of proB (9-11).

In vitro, proC is artificially converted to another active form, β-chelicerase C, *via* limited cleavage at the Phe[737]-Ile[738] bond by chymotrypsin (Fig. 1B) (12). β-Chelicerase C retains ~70% of the amidase activity of α-chelicerase C against a specific peptide substrate, whereas β-chelicerase C exhibits neither the LPS-binding activity nor the converting activity for proB because of the destruction of the LPS-binding site of proC by chymotryptic cleavage at the Tyr[40]-Cys[41] bond (11). ProB also interacts with

LPS with $K_d = 3.49 \times 10^{-9}$ M *via* an N-terminal domain named the clip domain (Fig. 1B), and several basic amino acid residues in the clip domain, including Lys[21], Lys[25], and Lys[38], play an important role in the LPS interaction (11, 13). In addition, a hydrophobic cavity located in the clip domain of proB has an important role for the efficiency of proteolytic activation by α-chelicerase C (13). ProCE also contains an N-terminal clip domain (Fig. 1B), whereas proCE has no LPS binding activity and its hydrophobic cavity proCE in the clip domain plays an essential role for its efficient activation by chelicerase B (13). Interestingly, proB evolutionarily lost the His-loop disulfide, which is one of the three conserved disulfide bonds located around the active site in trypsinogen/chymotrypsinogen-family members. We previously prepared a mutant named proB-murasame, equipped with a regenerated His-loop disulfide, which exhibits an order of magnitude higher k_{cat}/K_m value for specific peptide substrates than WT chelicerase B (7).

These horseshoe crab coagulation zymogens are stored in granules of granular hemocytes in hemolymph, accounting for 99% of all hemocytes (14), and are secreted *via* a protease-activated receptor and G protein-mediated signaling pathway in response to the stimulation of LPS (3). We previously reported an endogenous feed-back amplification mechanism for LPS-triggered exocytosis from granular hemocytes; an antimicrobial peptide, tachyplesin, one of the major components secreted from granular hemocytes, induces hemocyte exocytosis via a G protein-mediated signaling pathway and thereby amplifies LPS-triggered exocytosis, leading to efficient hemolymph coagulation (15).

In mammals, Ca^{2+} ions present at about 2 mM in plasma dramatically enhance the coagulation cascade by localizing serine protease zymogens of vitamin K-dependent coagulation factors on the surface of acidic phospholipids derived from activated platelets as a scaffold for the reaction; each of the vitamin K-dependent coagulation factors contains γ-carboxyglutamic acids at the N-terminal domain, which functions as a calcium-binding domain for the interaction with the scaffold (16). On other hand, horseshoe crab coagulation factors contain no γ-carboxyglutamic (1, 2), and the effects on Ca^{2+} ions on the horseshoe carb coagulation cascade triggered by LPS, an acidic scaffold, remain unknown.

91

Hemolymph in horseshoe crabs contains 10 mM Ca^{2+}, a higher Ca^{2+} concentration than found in human plasma (17). These findings suggested the existence of a mechanism by which Ca^{2+} ions amplify an LPS-triggered horseshoe crab coagulation cascade using three recombinant zymogens, i.e., wild-type (WT)-proC, WT-proB, and WT proCE.

In this study, we divided the LPS-triggered coagulation cascade into three stages and examined the effects of Ca^{2+} ions on each proteolytic activation: autocatalytic activation of WT proC on the surface of LPS into WT α-chelicerase C (Stage1); activation of WT proB on the surface of LPS into WT chelicerase B by WT α-chelicerase C (Stage 2); and activation of WT proCE into WT CE by chelicerase B independent of the presence or absence of LPS (Stage 3) (Fig. 1A). We also performed isothermal titration calorimetry (ITC) to clarify the interaction of Ca^{2+} ions with LPS or the recombinant zymogens from a thermodynamics point of view.

Experimental procedures

Materials

HEK293S GnTI⁻ cells were obtained from ATCC. LPS from *Salmonella minnesota* Re 595 (List Biological Laboratories, Campbell, CA), calcium chloride dihydrate (Nacalai Tesque, Kyoto, Japan), human serum albumin (HSA) (Fujifilm Wako Chemicals, Osaka, Japan), and trypsinogen from bovine pancreas (Sigma-Aldrich, St. Louis, MO) were purchased as the best commercially available products. An average relative molecular mass (Mr) of 2,500 for LPS was used for the determination of molecular concentrations. The protein concentration of trypsinogen (Mr= 24,000) was determined by using a Qubit 4 Fluorometer (Thermo Fisher Scientific, Boston, MA).

Cloning, mutagenesis, and expression of WT proC, WT proB, proB-murasame, and WT proCE

WT proC, WT proB, and WT proCE were subcloned into vector pCA7 and expressed in HEK293S GnTI⁻ cells, as described previously (11, 13, 18). ProB-murasame (A170C-proB) was constructed by inverse PCR and expressed in HEK293S GnTI⁻ cells, as described previously (7). These recombinant proteins were prepared as described previously (13, 18), and their concentrations were determined by using a Micro BCA™ protein assay kit (Thermo Fisher Scientific) or a Qubit 4 Fluorometer. The purified recombinants were analyzed by sodium dodecyl sulphate-polyacrylamide gel electrophoresis (SDS-PAGE) and Coomassie Brilliant Blue (CBB) staining (Supplemental Fig. S1).

Preparation of fully activated forms of the coagulation factors

Fully activated forms including WT α-chelicerase C (18), WT chelicerase B (11), chelicerase B-murasame (7), and WT CE (13) were prepared as previously reported. The resulting coagulation proteases were diluted with 20 mM Tris-HCl, pH 8.0, containing 150 mM NaCl and 0.1 mg/ml HSA. Their amidase activities were assayed at 37ºC using specific peptide substrates (Peptide Institute, Osaka,

Japan), i.e., *t*-butoxycarbonyl (Boc)-Val-Pro-Arg-4-methylcoumaryl-7-amide (MCA) for WT α-chelicerase C, Boc-Leu-Thr-Arg-MCA for WT chelicerase B or chelicerase B-murasame, and Boc-Leu-Gly-Arg-MCA for WT CE by monitoring fluorometrically using a 650-10S fluorescence spectrophotometer with excitation at 380 nm and emission at 440 nm (19). The end point assay of the amidase activity of each activated protease was determined by incubating with each specific peptide substrate for the indicated times at 37°C, and 10% acetic acid was added to terminate the reaction at the final concentration of 0.3%. The concentrations of generated CE were calculated from the specific amidase activity against Boc-Leu-Gly-Arg-MCA, as described previously (7, 13).

SDS-PAGE and western blotting

Samples were subjected to SDS-PAGE in 12% slab gels, and the gels were stained with CBB R-250. For western blotting, gels were transferred to a polyvinylidene difluoride membrane. After blocking with 5% non-fat dry milk for 30 min, the membrane was incubated with rabbit polyclonal antibody to the B-chain of chelicerase C (5), the B-chain of chelicerase B (11), or the H-chain of CE (20), and then horseradish peroxidase conjugated secondary antibody (Bio Rad Laboratories, Hercules, CA) was applied. The membranes were then developed with western Bright Sirius or ECL (Advansta, Menlo Park, CA). Images were obtained by an Omega Lum G imaging system (Aplegen Life Sciences, San Francisco, CA).

ITC analysis of the interaction of Ca^{2+} ions with the recombinant zymogens and trypsinogen

ITC experiments were performed at 25°C (298 K) using an auto-iTC 200 (Malvern Panalytical Worcestershire, UK). Each recombinant zymogen or trypsinogen was treated with 100 mM EDTA and dialyzed extensively against 20 mM HEPES-NaOH, pH 8.0, containing 150 mM NaCl. Calcium chloride dihydrate was dissolved in the buffer remaining in the beaker after completion of dialysis. For ITC for the interaction of Ca^{2+} ions with LPS, LPS or calcium chloride dihydrate was dissolved 20 mM

HEPES-NaOH, pH 8.0, containing 150 mM NaCl. A 0.4 microliter aliquot followed by multiple 2 μl aliquots of the solution containing Ca^{2+} ions were injected successively into 200 μl of the protein or LPS solution every 3 min for a total of 20 cycles. The heat generated by the mixing itself was measured by injecting the Ca^{2+} solution into the dialysis buffer, and integrated heat effects were analyzed by fitting a single-site binding model using Origin 7 (OriginLab, Northampton, MA). The fitted data yielded the association constant (K_a), the number of binding sites on the protein (n), the enthalpy of binding (ΔH), and the entropy of binding (ΔS).

Statistical analysis

Statistical analysis was performed by paired t-tests, and P-values < 0.05 were considered to be statistically significant.

Results

Effects of Ca²⁺ ions on the LPS-triggered cascade reaction reconstituted with the three recombinant zymogens in the presence of LPS

We first investigated the effect of Ca^{2+} ions on the cascade reaction involving the three recombinant zymogens—WT proC, WT proB, and WT proCE—in the presence of LPS (Fig. 2). The production of WT CE in the cascade trigged by LPS was clearly higher in the presence of 5 mM Ca^{2+} (Fig. 2A, *solid line*) than in the absence of Ca^{2+} ions (Fig. 2A, *dotted line*). The possible incorporation of Ca^{2+} ions into the recombinant zymogens during their preparations was investigated by adding 1 mM EDTA to the reaction mixture, and the reaction progress curve with the addition of EDTA was consistent with that without Ca^{2+} ions (Fig. 2A, *dashed line*), indicating that no Ca^{2+} ions were incorporated into the recombinant zymogens during their purification processes. The concentration of WT CE produced 3 min after the addition of LPS was estimated from the specific amidase activity of WT CE (Fig. 2B), indicating that the concentration of WT CE produced in the presence of 5 mM Ca^{2+} increased 2-fold compared to that in the absence of Ca^{2+} ions.

Effect of Ca²⁺ ions on Stage 1, the autocatalytic activation of WT proC on the surface of LPS

We first investigated the effects of Ca^{2+} ions on Stage 1, the autocatalytic activation of WT proC on LPS. After 30-min autocatalytic activation of WT proC by LPS at concentrations ranging from 1.0 nM~100 μM in the presence or the absence of Ca^{2+} ions, the amidase activity of WT α-chelicerase C produced was measured using the specific peptide substrate (Fig. 3A). WT proC was autocatalytically activated in the absence of Ca^{2+} ions (Fig. 2A, *open circles*), showing a bell-shaped activation pattern with the highest activity at 1.0 μM LPS at the molar ratio of [LPS] : [WT proC] = 40 : 1 under the conditions employed. On the other hand, WT proC was autocatalytically activated in the presence of 5 mM Ca^{2+}. Unexpectedly, the amidase activity of WT α-chelicerase C produced was reduced to about 1/2 by the

96

addition of 5 mM Ca^{2+}, compared with that produced in the absence of Ca^{2+} ions, although the dependence of the amidase activity on LPS concentration increased in the presence of LPS concentrations up to 10 μM.

Moreover, to examine the effect of Ca^{2+} ions on the autocatalytic conversion of WT proC on the surface of LPS to WT α-chelicerase C, 50 nM of WT proC was incubated with 2 μM of LPS in the presence or absence of Ca^{2+} ions. The time course of proteolytic conversion of WT proC to WT α-chelicerase C was then evaluated by the appearance of the B chain of WT α-chelicerase C on western blotting (Fig. 3B), and the relative densities of the B chain and the L chain were analyzed (Fig. 3C). The B chain appeared more slowly in the presence of 5 mM Ca^{2+} (Fig. 3B, *right panel* and Fig. 3C, *closed circles*) than in the absence of Ca^{2+} ions (Fig. 3B, *left panel* and Fig. 3C, *open circles*).

In addition, after the autocatalytic activation of WT ProC under the same conditions as shown in Fig. 3B, the amidase activities of WT α-chelicerase C at the indicated time points were assayed using its specific peptide substrate. We found that the amidase activity of WT α-chelicerase C produced in the presence of 5 mM Ca^{2+} was significantly reduced, compared to that of WT α-chelicerase C produced in the absence of Ca^{2+} (Fig. 3D). These results indicate that Ca^{2+} ions do not enhance the proteolytic conversion at Stage 1, the autocatalytic activation of WT proC on the surface of LPS into WT α-chelicerase C.

Effect of Ca^{2+} ions on Stage 2, the activation of WT proB on the surface of LPS by WT α-chelicerase C

We next investigated effects of Ca^{2+} ions on the activation of WT proB on the surface of LPS by α-chelicerase C. It was not possible to conduct quantitative measurement of the time course of the amidase activity of WT chelicerase B using its specific peptide substrate, because the k_{cat}/K_m value of WT chelicerase B against the specific peptide substrate (k_{cat}/K_m = 5,300 $M^{-1}s^{-1}$) is orders of magnitude lower than those of WT α-chelicerase C (k_{cat}/K_m = 370,000 $M^{-1}s^{-1}$) and WT CE (k_{cat}/K_m = 3,600,000 $M^{-1}s^{-1}$)

(13). Therefore, the time course of proteolytic conversion of WT proB to WT chelicerase B by WT α-chelicerase C was evaluated by the appearance of the B chain of WT chelicerase B on western blotting (Fig. 4A), and the relative density of the B chain was analyzed (Fig. 4B). The appearance of the B chain of WT chelicerase B occurred significantly more quickly in the presence of 5 mM Ca^{2+} (Fig. 4A, *right panel* and Fig. 4B, *closed circles*) than that of the B chain in the absence of Ca^{2+} ions (Fig. 4A, *left panel* and Fig. 4B, *open circles*). These results suggest that Ca^{2+} ions dramatically enhance the conversion of WT proB on the surface of LPS to WT chelicerase B by WT α-chelicerase C.

Effect of Ca^{2+} ions on Stage 3, the activation of WT proCE by WT chelicerase B

Next, we investigated the effects of Ca^{2+} ions on the activation of proCE into CE by WT chelicerase B. The conversion of WT proCE to CE by WT chelicerase B in the presence or absence of Ca^{2+} was measured using its specific peptide substrate. The results showed that the time course of the amidase activity of the produced WT CE was not affected by the presence or absence of Ca^{2+} ions (Fig. 5A), and no change was observed in the molar concentration of WT CE after 2 min of incubation in the presence or absence of Ca^{2+} ions, clearly indicating that the proteolytic activation at Stage 3, the activation of WT proCE into CE by WT chelicerase B, was not affected by the presence or absence of Ca^{2+} ions.

Effect of Ca^{2+} ions on the amidase activity of WT α-chelicerase C, WT CE, and chelicerase B-murasame

Here, we examined the effects of Ca^{2+} ions on the amidase activity of chelicerase B-murasame instead of WT chelicerase B, because chelicerase B-murasame exhibits an order of magnitude higher k_{cat}/K_m value for specific peptide substrates compared to WT chelicerase B (7). As a result, addition of 5 mM Ca^{2+} had no effects on any of the amidase activities of WT α-chelicerase C, WT CE, or chelicerase B-murasame against their specific peptide substrate (Fig. 6).

ITC for the interaction of the recombinant zymogens or LPS with Ca²⁺ ions

We performed ITC to clarify the interaction of the coagulation zymogens, i.e., WT proC, WT proCE, and proB-murasame, with Ca^{2+} ions. Here, proB-murasame was used instead of WT proB because the expression of WT proB was much lower than that of proB-murasame, and not sufficient for the ITC measurement. First, as a positive control, we conducted an ITC analysis of the interaction between trypsinogen and Ca^{2+} ions. The ITC data for the interaction fit a single-site binding model with several parameters ($K_a = 7.7 \times 10^6$ M⁻¹, n = 0.44, $\Delta H = -6.60$ kcal/mol, $-T\Delta S = -2.59$ kcal/mol, and $\Delta G = -9.19$) (Supplemental Fig. S2). In contrast, no obvious interaction was detected between each of the three recombinant zymogens and Ca^{2+} ions by ITC (Supplemental Fig. S2).

Next, we conducted ITC to clarify the interaction between LPS at 100 μM and Ca^{2+} ions. However, the molar concentration of LPS was calculated as a monomer in solution, not as an aggregate. A clear interaction was observed between LPS and Ca^{2+} ions with parameters ($K_a = 4.7 \times 10^4$ M⁻¹, n = 0.26, $\Delta H = -3.50$ kcal/mol, $-T\Delta S = -2.80$ kcal/mol, and $\Delta G = -6.30$) (Fig. 7). Based on these parameters, the interaction between LPS and Ca^{2+} ions that contribute to the binding may consist of both enthalpy-driven interaction with high specificity and entropy-driven interactions with low specificity.

Discussion

In this study, we found that Ca^{2+} ions enhanced the horseshoe crab coagulation cascade reconstituted by three recombinant zymogens, namely, WT proC, WT proB, and WT proCE, leading to the increased production of WT CE (Fig. 2). To investigate which step of the cascade reaction was affected by the addition of Ca^{2+} ions, the cascade was divided into the three stages for evaluation: autocatalytic activation of WT proC on LPS (Stage 1); activation of WT proB on LPS by WT α-chelicerase C (Stage 2); and activation of WT proCE by chelicerase B (Stage 3). We found that Ca^{2+} ions enhanced Stage 2, i.e., the proteolytic conversion of proB on the surface of LPS to chelicerase B by WT α-chelicerase, but not the other two proteolytic activation Stages 1 (Fig. 3) and 3 (Fig. 5). In addition, we confirmed that Ca^{2+} ions had no effect on the amidase activities of the fully activated proteases—i.e., WT α-chelicerase C, WT chelicerase B and WT CE—against their peptide substrates in the absence of LPS (Fig. 6).

To clarify the interaction of Ca^{2+} ions with the recombinant zymogens or LPS, ITC was performed. We found that LPS clearly interacted with Ca^{2+} ions at the association constant of $K_a = 4.7 \times 10^4$ M^{-1} (Fig. 7) (Supplemental Fig. S2). Considering the concentration of Ca^{2+} ions in the horseshoe crab hemolymph (10 mM) (17), an interaction between LPS and Ca^{2+} ions is quite possible under physiological conditions. It should be noted that the LPS concentration used for the ITC measurements (100 μM) was much greater than that used for the proteolytic activation in Stage 1 (2 μM) (Fig. 3B) or Stage 2 (160 nM) (Fig. 4A). Therefore, under conditions used here, which exceeded the critical aggregation concentration of LPS (4 μM for LPS from *S. minnesota* Re 595) (21), it might be difficult to obtain correct thermodynamic parameters for the interaction between LPS and Ca^{2+} ions, because LPS is presumed to form various types of aggregates in solution over the critical aggregation concentration.

Crystal structural analysis showed that trypsinogen or trypsin has a Ca^{2+}-binding site at the surface loop that is designated the 70–80 loop in chymotrypsinogen numbering, and this site is conserved among

trypsinogen/chymotrypsinogen-family members in mammals and invertebrates, and the acidic side chains of Glu^{70} and Glu^{80} are important for Ca^{2+} binding (Fig. 8A) (22, 23). Our ITC measurements showed a strong interaction between trypsinogen with Ca^{2+} ions with $K_a = 7.7 \times 10^6 \, M^{-1}$, but not between any of the recombinant zymogens and Ca^{2+} ions (Supplemental Fig. S2). Interestingly, the conserved Glu^{70} is replaced with Lys and Gly in proC and proB, respectively, although the important Glu^{70} is conserved in proCE (Fig. 8B). Figure 9 shows three-dimensional structures for the protease domains of proC, proB and proCE predicted by AlphaFold (24, 25). The 70–80 loop structure predicted for each of the coagulation zymogens occupies almost the same surface area as the 70–80 loop determined by the crystal structure of trypsinogen, but the structures around the 70–80 loop of the coagulation zymogens are significantly different from that of trypsin, especially for the protease domains of proC and proB. (Fig. 9).

Interestingly, the efficiency of autocatalytic activation of proC on LPS was decreased by the addition of Ca^{2+} ions, suggesting that Ca^{2+} ions suppress the autocatalytic activation of WT proC on the surface of LPS into α-chelicerase C (Fig. 3). Lam *et al*. reported that the surface of LPS micelles is coated by divalent cations or other positively charged substances such as basic antimicrobial peptides (26). Therefore, Ca^{2+} ions might inhibit the interaction of proC with LPS via its N-terminal LPS-binding triplet, Arg^{36}-Trp^{37}-Arg^{38} (1, 4). However, the suppression of the autocatalytic activation of WT proC on LPS in the presence of Ca^{2+} ions at Stage 1 should be counteracted by the increased proteolytic activation of WT proB on LPS by WT α-chelicerase C in the presence of Ca^{2+} ions at Stage 2, because Ca^{2+} ions enhance the overall cascade reconstituted by the three recombinant zymogens (Fig. 2).

Figure 10 shows three-dimensional structures for the LPS-binding Cys-rich domain of proC (*left panel*) and the LPS-binding clip domain of proB (*right panel*), predicted by AlphaFold (24, 25). The LPS-binding triplet composed of Arg^{36}-Trp^{37}-Arg^{38} of proC plays an important role for LPS binding (1, 4). We proposed previously that the side chains of the Arg^{36} and Arg^{38} residues interact with glucosamine I-1-phospahte in the lipid A portion of LPS, and that the side chain of Trp^{37} interacts with a hydrophobic

region of the lipid A portion or may interact with the indole ring of the glucosamine I by stacking (4). The clip domain of proB plays a key role in LPS binding, and several basic amino acid residues in the clip domain, including Lys[21], Lys[25], and Lys[38], have an important role for the LPS interaction (13). In addition, a hydrophobic cavity located in the clip domain also has an important role for the efficiency of proteolytic activation of proB on LPS by α-chelicerase C (13). Through the binding of Ca^{2+} ions to LPS, the interaction between proC and proB, both located on the surface of LPS, may become more favorable, which would enhance the efficiency of activation of proB by α-chelicerase C—that is, the cascade reaction may be accelerated by the stage 1 and stage 2 reactions occurring simultaneously in very close proximity to the LPS surface (Fig. 11). Based on the present findings, we concluded that LPS bound with Ca^{2+} ions facilitates the chain reaction of the cascade as a more efficient scaffold than LPS itself.

References

1. Kawabata, S. and Shibata, T. (2022) New insights into the hemolymph coagulation cascade of horseshoe crabs initiated by autocatalytic activation of a lipopolysaccharide-sensitive zymogen. *Dev. Comp. Immunol.* **135**, 104491

2. Kawabata, S., and Muta, T. (2010) Sadaaki Iwanaga: discovery of the lipopolysaccharide- and b-1,3-D-glucan-mediated proteolytic cascade and unique proteins in invertebrate immunity. *J. Biochem.* **147**, 611–618

3. Ariki, S., Koori, K., Osaki, T., Motoyama, K., Inamori, K., and Kawabata, S. (2004) A serine protease zymogen functions as a pattern-recognition receptor for lipopolysaccharides. *Proc. Natl. Acad. Sci. U. S. A.* **101**, 953–958

4. Koshiba, T., Hashii, T., and Kawabata, S. (2007) A structural perspective on the interaction between lipopolysaccharide and factor C, a receptor involved in recognition of gram-negative bacteria. *J. Biol. Chem.* **282**, 3962–3967

5. Shibata, T., Kobayashi, Y., Ikeda, Y., and Kawabata, S. (2018) Intermolecular autocatalytic activation of serine protease zymogen factor C through an active transition state responding to lipopolysaccharide. *J. Biol. Chem.* **293**, 11589–11599

6. Nakamura, T., Horiuchi, T., Morita, T., and Iwanaga, S. (1986) Purification and properties of intracellular clotting factor, factor B, from horseshoe crab (*Tachypleus tridentatus*) hemocytes. *J. Biochem.* **99**, 847-857

7. Yamashita, K., Takeshita, N., Arita, A., Shibata, T., Kobayashi, Y., and Kawabata, S. (2021). A mutant equipped with a regenerated disulfide for the missing His loop of a serine protease zymogen in the horseshoe crab coagulation cascade. *J. Biochem.* **170**, 489–500

8. Kawasaki, H., Nose, T., Muta, T., Iwanaga, S., Shimohigashi, Y., and Kawabata, S. (2000) Head-to-tail polymerization of coagulin, a clottable protein of the horseshoe crab. *J. Biol. Chem.* **275**, 35297–

35301

9. Morita, T., Tanaka, S., Nakamura, T., and Iwanaga, S. (1981) A new (1 → 3)-β-ᴅ-glucan-mediated coagulation pathway found in limulus amebocytes, *FEBS Letters*. **129**, 318–321

10. Muta, T., Oda, T., and Iwanaga, S. (1993) Horseshoe crab coagulation factor B. A unique serine protease zymogen activated by cleavage of an Ile-Ile bond. *J. Biol. Chem.* **268**, 21384–21388

11. Kobayashi, Y., Takahashi, T., Shibata, T., Ikeda, S., Koshiba, T., Mizumura, H., Oda, T., and Kawabata, S. (2015) Factor B is the second lipopolysaccharide-binding protease zymogen in the horseshoe crab coagulation cascade. *J. Biol. Chem.* **290**, 19379–19386

12. Tokunaga, F., Nakajima, H., and Iwanaga, S. (1991) Further studies on lipopolysaccharide-sensitive serine protease zymogen (factor C): its isolation from *Limulus polyphemus* hemocytes and identification as an intracellular zymogen activated by α-chymotrypsin, not by trypsin. *J. Biochem*. **109**, 150-1578.

13. Yamashita, K., Shibata, T., Takahashi, T., Kobayashi, Y., and Kawabata, S. (2020) Roles of the clip domains of two protease zymogens in the coagulation cascade in horseshoe crabs. *J. Biol. Chem.* **295**, 8857–8866

14. Toh, Y., Mizutani, A., Tokunaga, F., Muta, T., and Iwanaga, S. (1991) Morphology of the granular hemocytes of the Japanese horseshoe crab *Tachypleus tridentatus* and immunocytochemical localization of clotting factors and antimicrobial substances. *Cell Tissue Res*. **266**, 137–147

15. Ozaki, A., Ariki, S., and Kawabata, S. (2005) An antimicrobial peptide tachyplesin acts as a secondary secretagogue and amplifies lipopolysaccharide-induced hemocyte exocytosis. *FEBS J*. **272**, 3863-3871

16. O'Donnell, J. S., O'Sullivan, J. M., and Preston, R. J. S. (2019) Advances in understanding the molecular mechanisms that maintain normal haemostasis. *British J. Haematol*. **186**, 24-36

17. Robertson, J.D. (1970) Osmotic and ionic regulation in the horseshoe crab *Limulus* polyphemus (Linnaeus). *Biol. Bull*. **138**, 157–183

18. Kobayashi, Y., Shiga, T., Shibata, T., Sako, M., Maenaka, K., Koshiba, T., Mizumura, H., Oda, T., and Kawabata, S. (2014) The N-terminal Arg residue is essential for autocatalytic activation of a lipopolysaccharide-responsive protease zymogen. *J. Biol. Chem.* **289**, 25987–25995

19. Kawabata, S., Miura, T., Morita, T., Kato, H., Fujikawa, K., Iwanaga, S., Takada, K., Kimura, T., and Sakakibara, S. (1988) Highly sensitive peptide-4-methylcoumaryl-7-amide substrates for blood-clotting proteases and trypsin. *Eur. J. Biochem.* **172**, 17–25

20. Mizumura, H., Ogura, N., Aketagawa, J., Aizawa, M., Kobayashi, Y., Kawabata, S., and Oda, T. (2017) Genetic engineering approach to develop next-generation reagents for endotoxin quantification. *Innate Immun.* **23**, 136–146

21. Aurell, C. A. and Wistrom, A. O. (1998) Critical aggregation concentration of Gram-negative bacterial lipopolysaccharide (LPS). *Biochem. Biophys. Res. Commun*. **253**, 119–123

22. Bode, W., and Schwager, P. (1975) The single calcium-binding site of crystallin bovine beta-trypsin. *FEBS letters*. **56**, 139–143

23. Goettig, P., Brandstetter, H., and Magdolen, V. (2019) Surface loops of trypsin-like serine proteases as determinants of function. *Biochimie*. **166**, 52–76

24. Jumper, J, Evans, R., Pritzel, A., Green, T., Figurnov, M., Ronneberger, O., Tunyasuvunakool, K., Bates, R., Židek, A., Potapenko, A., Bridgland, A., Meyer, C., Kohl, S.A.A., Ballard, A.J., Cowie, A., Romera-Paredes, B., Nikolov, S., Jain, R., Adler, J., Back, T., Petersen, S., Reiman, D., Ellen Clancy, E., Zielinski, M., Steinegger, M., Pacholska, M., Tamas Berghammer, T., Sebastian Bodenstein, S., Silver, D., Vinyals, O., Senior, A.W., Kavukcuoglu, K., Kohli, P., and Hassabis, D. (2021) Highly accurate protein structure prediction with AlphaFold. *Nature*. **596**, 583–592

25. Varadi, M., Anyango, S., Deshpande, M., Nair, S., Natassia, C., Yordanova, G., Yuan, D., Stroe, O., Wood, G., Laydon, A., Židek, A., Green, T., Tunyasuvunakool, K., Petersen, S., Jumper, J., Clancy, E., Green, R., Vora, A., Lutfi, M., Figurnov, M., Cowie, A., Hobbs, N., Kohli, P., Kleywegt, G., Birney, E., Hassabis, D., and Velankar, S. (2022) AlphaFold protein structure database: massively

expanding the structural coverage of protein-sequence space with high-accuracy models. *Nucleic Acids Res*. **50**, D439–D444

26. Lam, N. H., Ma, Z., and Ha, B. Y. (2014) Electrostatic modification of the lipopolysaccharide layer: competing effects of divalent cations and polycationic or polyanionic molecules. *Soft matter*. **10**, 7528–7544

27. Muta, T., Miyata, T., Misumi, Y., Tokunaga, F., Nakamura, T., Toh, Y., Ikehara, Y., and Iwanaga, S. (1991) *Limulus* factor C. An endotoxin-sensitive serine protease zymogen with a mosaic structure of complement-like, epidermal growth factor-like, and lectin-like domains. *J. Biol. Chem.* **266**, 6554–6561

28. Muta, T., Hashimoto, R., Miyata, T., Nishimura, H., Toh, Y., and Iwanaga, S. (1990) Proclotting enzyme from horseshoe crab hemocytes. cDNA cloning, disulfide locations, and subcellular localization. *J. Biol. Chem.* **265**, 22426–22433

29. Seki, N., Muta, T., Oda, T., Iwaki, D., Kuma, K., Miyata, T., and Iwanaga, S. (1994) Horseshoe crab (1,3)-β-D-glucan-sensitive coagulation factor G. *J. Biol. Chem.* **269**, 1370–1374

30. Piao, S., Song, Y., Kim, J. H., Park, S. Y., Park, J. W., Lee, B. L., Oh, B., and Ha, N. (2005) Crystal structure of a clip-domain serine protease and functional roles of the clip domains. *EMBO J.* **24**, 4404–4414

31. Kellenberger, C., Leone, P., Coquet, L., Jouenne, T., Reichhart, J. M., and Roussel, A. (2011) Structure-function analysis of grass clip serine protease involved in *Drosophila* Toll pathway activation. *J. Biol. Chem.* **286**, 12300–12307

Figure legends

Fig. 1. The proteolytic coagulation cascade of horseshoe crab hemolymph. (**A**) The coagulation cascade was independently triggered by LPS and β-1,3-D-glucan. The LPS-triggered proteolytic cascade was divided into three proteolytic stages: Stage 1, autocatalytic activation of proC on LPS; Stage 2, activation of proB by α-chelicerase C on the surface of LPS; Stage 3, activation of proCE by chelicerase B independent of the presence or absence of LPS. (**B**) The domain structures of proC (27), proB (10), and proCE (28), and their disulfide bridges are shown schematically. The *N*-linked sugar binding sites of each zymogen are shown by *diamonds*. The cleavage sites required for activation of each protein are indicated by *closed triangles*, and the prior cleavage site for activation in proB is indicated by an *open triangle*.

Fig. 2. Effects of Ca^{2+} ions on the LPS-triggered proteolytic cascade reconstituted with the recombinant proteins WT proC, WT proB, and WT proCE in the presence or absence of Ca^{2+}. (**A**) A reaction mixture containing 10 nM each of WT proC, WT proB, and WT proCE was incubated at 37°C in the presence (5 mM Ca^{2+}, *solid line*), absence of Ca^{2+} ions (*dotted line*) or in the presence of 1 mM EDTA (*dashed line*). The proteolytic cascade was initiated by adding 1 μM LPS, and the resulting amidase activity of the generated CE was fluorometrically monitored using Boc-Leu-Gly-Arg-MCA. Data are representative of three independent experiments. (**B**) The concentration of AMC generated after 3 min of incubation in the presence (5 mM Ca^{2+}) or absence of Ca^{2+} ions, as shown in Fig. 2 (A), was converted into the concentration of CE using its specific activity as described in the "*Experimental procedures*". Data are the means ± standard error of the mean (SEM) of three independent experiments. **, $P < 0.01$.

Fig. 3. Effects of Ca²⁺ ions on Stage 1, the autocatalytic activation of WT proC on the surface of LPS. (A) 25 nM WT proC was incubated with various concentrations of LPS (1 nM–100 μM) for 30 min at 37°C in the presence (5 mM Ca²⁺, *closed circles*) or absence of Ca²⁺ ions (*open circles*). The vertical axis indicates the relative amidase activities of α-chelicerase generated autocatalytically using Boc-Val-Pro-Arg-MCA. Data are the means ± SEM of three independent experiments. **(B)** 50 nM WT proC was incubated with 2 μM LPS at 37°C in the presence (5 mM Ca²⁺, *right panel*) or absence of Ca²⁺ (*left panel*). Aliquots at the indicated reaction times were subjected to western blotting using the anti-B chain of α-chelicerase C antibody. Data are representative of three independent experiments. L, the light chain of WT proC; B, the B chain of WT α-chelicerase C. The L chain appears as two bands because the glycosylation of the L chain is partial (18). **(C)** The band intensities of L and B chains in the presence (5 mM Ca²⁺, *closed circles*) or absence of Ca²⁺ (*open circles*) as shown in Fig. 3B were analyzed using ImageJ software. The vertical axis shows the percentage of B chain appearance. Data are the means ± SEM of three independent experiments. **(D)** 50 nM WT proC was incubated with 1 μM LPS in the presence (5 mM Ca²⁺, *closed circles*) or absence (*open circles*) of Ca²⁺ ions at 37°C. The amidase activities of the resulting WT α-chelicerase C at the indicated times were analyzed using Boc-Val-Pro-Arg-MCA. The vertical axis indicates the relative activities. Data are the means ± SEM of three independent experiments.

Fig. 4. Effects of Ca²⁺ ions on Stage 2, the activation of WT proB on the surface of LPS by WT α-chelicerase C. (A) 50 nM WT proB was incubated with 4 nM WT α-chelicerase C in the presence of 160 nM LPS at 37°C in the presence (5 mM Ca²⁺, *right panel*) or absence (*left panel*) of Ca²⁺ ions. Aliquots at the indicated reaction times were subjected to western blotting using the anti-B chain of chelicerase B antibody. Data are representative of three independent experiments. S, the single chain of WT proB; H, the heavy chain of WT proB; B, the B chain of WT chelicerase B. **(B)** The band intensities of S, H, and B chains in the presence (5 mM Ca²⁺, *closed circles*) or absence (*open circles*) of Ca²⁺ ions

as shown in Fig. 3B were analyzed by ImageJ software. The vertical axis shows the appearance rate of B chain. Data are the means ± SEM of three independent experiments. *, $P < 0.05$; **, $P < 0.01$.

Fig. 5. Effects of Ca²⁺ ions on Stage 3, the activation of WT proCE by WT chelicerase B. (**A**) 10 nM WT proCE was incubated with 10 nM WT chelicerase B at 37°C in the presence (5 mM Ca^{2+}, *solid line*) or absence (*dotted line*) of Ca^{2+} ions, and the amidase activity of CE generated was fluorometrically monitored using Boc-Leu-Gly-Arg-MCA. Data are representative of three independent experiments. (**B**) The concentration of AMC generated after 2 min of incubation in the presence or absence of Ca^{2+} ions shown in Fig. 5 (A) was converted into the concentrations of CE using its specific activity. Data are the means ± SEM of three independent experiments.

Fig. 6. Effects of Ca²⁺ ions on the amidase activity of WT α-chelicerase C, WT chelicerase B-murasame, or WT CE against their specific peptide substrates. WT α-chelicerase C was incubated with Boc-Val-Pro-Arg-MCA, chelicerase B-murasame was incubated with Boc-Leu-Thr-Arg-MCA, and WT CE was incubated with Boc-Leu-Gly-Arg-MCA, in the presence (5 mM) or absence of Ca^{2+} ions for 5 min. Units represent the amount of synthetic substrate (μmol) digested per min. Data are the means ± SEM of three independent experiments.

Fig. 7. ITC for the interaction of LPS with Ca²⁺ ions. ITC was performed by injecting 2 mM of Ca^{2+} ions into 100 μM of LPS at 3 min intervals. The upper panel shows a representative thermogram and the lower panel shows the integrated amounts of heat.

Fig. 8. Structural comparison of the Ca²⁺-binding loop (the 70–80 loop) of trypsinogen with those of the horseshoe crab coagulation factors and other serine protease zymogens. (**A**) The crystal structure of bovine trypsinogen (22, 23). The catalytic triad composed of His⁵⁷, Asp¹⁰², and Ser¹⁹⁵ in

109

chymotrypsinogen numbering is indicated in *orange*, and the 70–80 loop is indicated in *green*. (**B**) The sequence alignment of the 70–80 loop of *Tt*-proC (27), *Tt*-proB (10), *Tt*-proCE (28), and the *Tt*-proG β-subunit (29) and the other serine proteases zymogens—i.e., *Hd*-PPAF-II (30), *Dm*-Grass (31), *Hs*-factor-IX (23), *Hs*-factor VII (23), and *Bt*-trypsinogen (22). *Tt*, *Tachypleus tridentatus*; *Hd*, *Holotrichia diomphalia*; *Dm*, *Drosophila melanogaster*; *Hs*, *Homo sapiens*; *Bt*, *Bos taurus*. The E^{70} and E^{80} residues in chymotrypsinogen numbering are indicated by *bold* letters.

Fig. 9. Predicted structures for the protease domains of WT proC, WT proB, and WT proCE. The protease domains of proC, proB, and proCE were predicted by AlphaFold (24, 25). The catalytic triad and the 70-80 loop of each zymogen are indicated in *orange* and *green*, respectively.

Fig. 10. Predicted structure for the LPS-binding Cys-rich domain in proC and the LPS-binding clip domain in proB. The two LPS-binding domains, the LPS-binding Cys-rich domain in proC (*left panel*) and the LPS-binding clip domain in proB (*right panel*), were predicted by AlphaFold (24, 25). The side chains of possible amino acid residues that interact with LPS in the Cys-rich domain (4) or the clip domain (13) are indicated in blue.

Fig. 11. The surface created by the interaction of LPS with Ca^{2+} ions provides an effective scaffold for the activation of proB by α-chelicerase C. In the absence of Ca^{2+} ions (*upper panel*), proC on LPS is autocatalytically converted to α-chelicerase C (*capital letter C*), and the resulting α-chelicerase C activates proB on LPS into chelicerase B (*capital letter B*). Then, chelicerase B activates proCE into CE. The proteolytic activation of Stages 1 and 2 occur independently on the surface of LPS. In the presence of Ca^{2+} ions (*lower panel*), the activation of proB by α-chelicerase C may be accelerated by the stage 1 and stage 2 reactions occurring simultaneously in very close proximity to the LPS surface.

Supplemental figure legends

Fig. S1. A typical pattern of SDS-PAGE for the recombinant proteins. The recombinant proteins WT proC, WT proB, proB-murasame, and WT proCE were subjected to SDS-PAGE and stained with CBB R-250. The letters, S, H, and L, indicate the single chain, the heavy chain, and the light chain of each recombinant protein, respectively. Depending on preparation lots of WT proB or ProB-murasame, the two-chain-form zymogen (the H and L chains) of proB cleaved at the site 1 may be present in the preparation

Fig. S2. ITC analysis of the interaction of trypsinogen, WT proC, proB-murasame, or WT proCE with Ca^{2+} ions. ITC was performed by injecting 100 μM Ca^{2+} into 15 μM trypsinogen, 50 μM Ca^{2+} into 5 μM WT proC, 100 μM Ca^{2+} into 8 μM proB-murasame, or 1 mM Ca^{2+} into 50 μM WT proCE at 3 min intervals. Each panel shows a representative thermogram (*upper panel*) and the integrated amounts of heat (*lower panel*).

Figure 1A

B

ProC

Cys-rich domain

LPS-binding site

36
-R-W-R-

737
-F-I-

The cleavage site
for activation

ProB

Clip

Serine protease
domain

LPS-binding site

103
-R-S-

The cleavage site 1

124
-I-I-

The cleavage site 2
for activation

ProCE

Clip

Serine protease
domain

98
-R-I-

The cleavage site for activation

Figure 1B

113

Figure 2

Figure 3

Figure 4

A

B
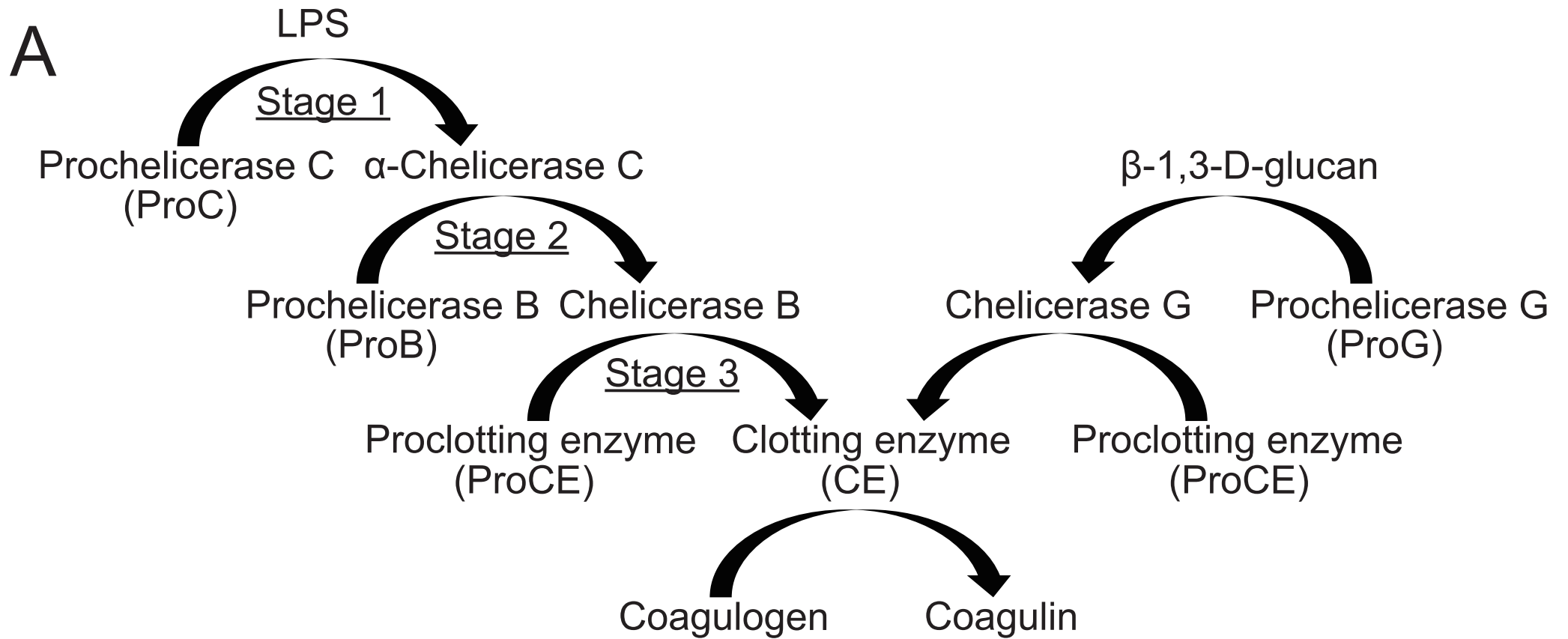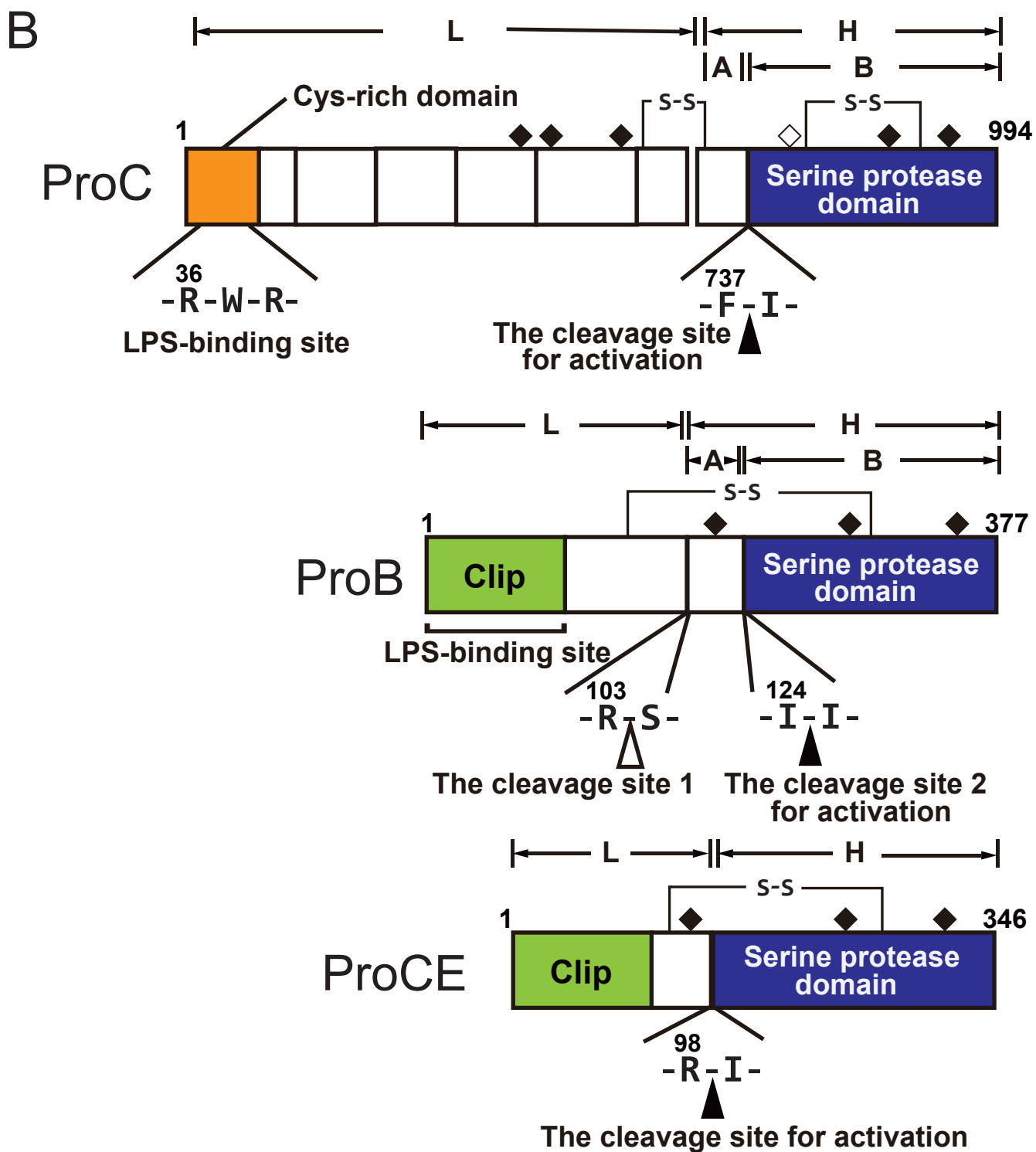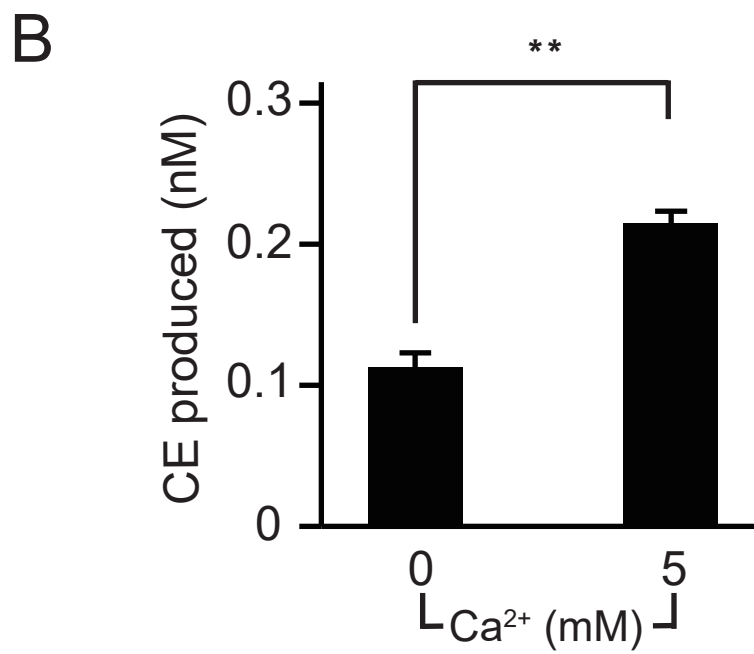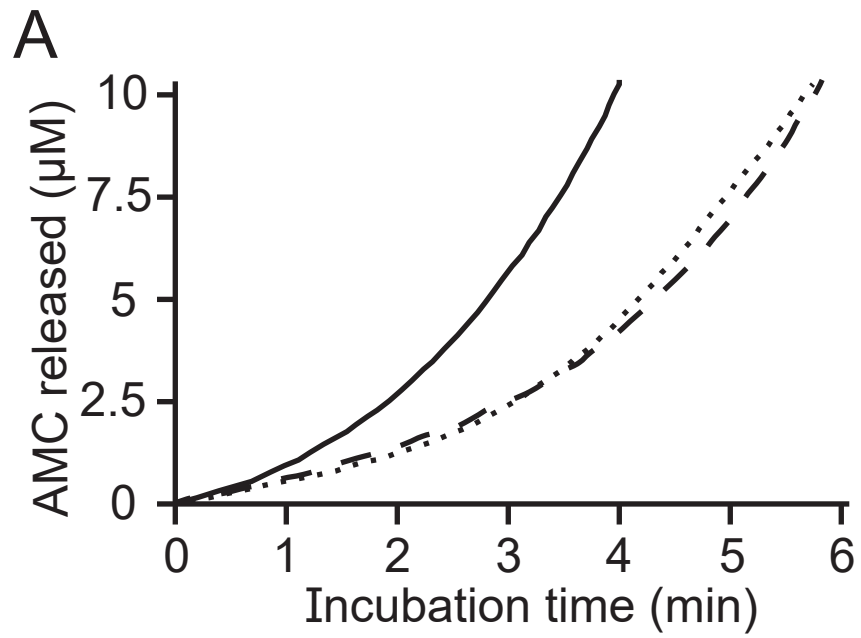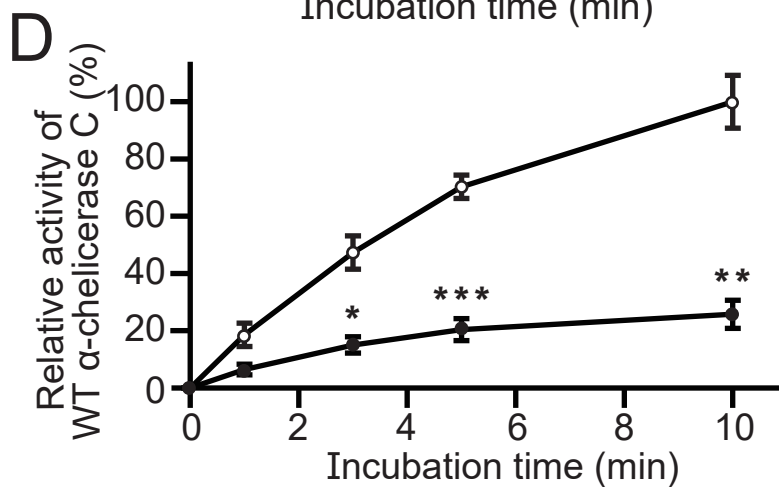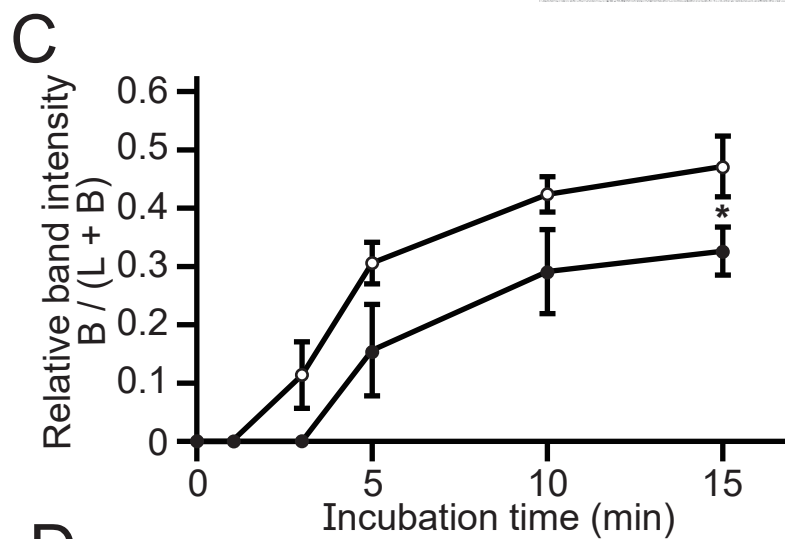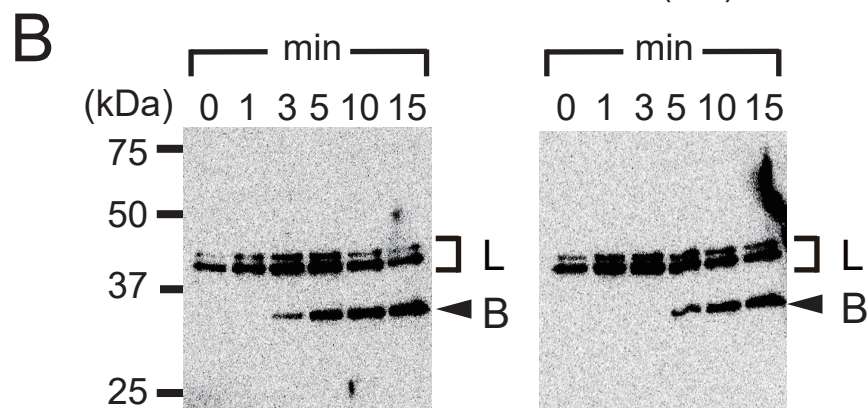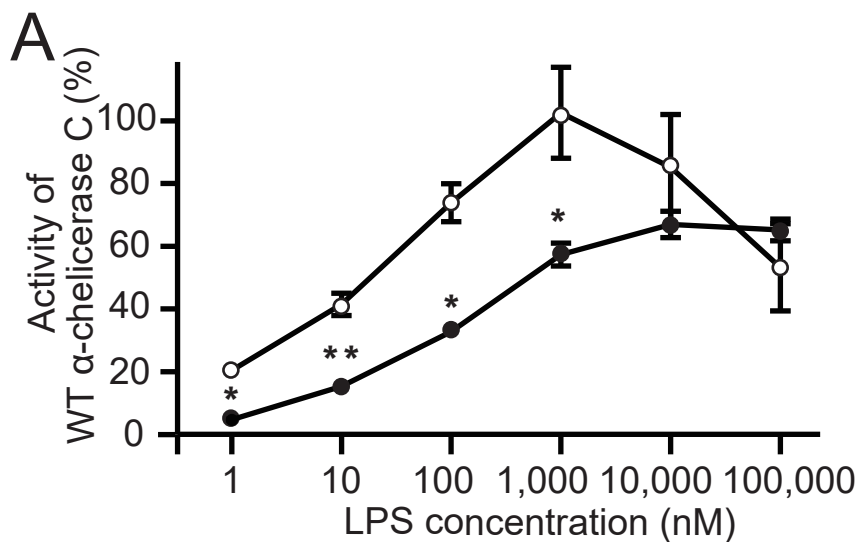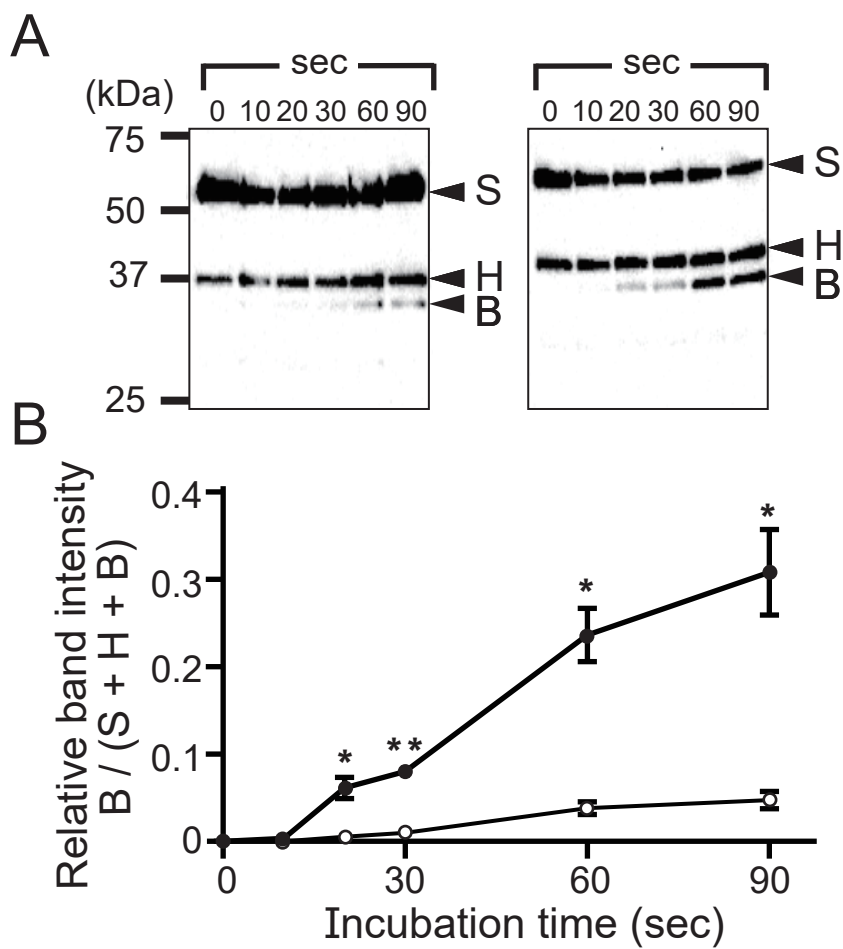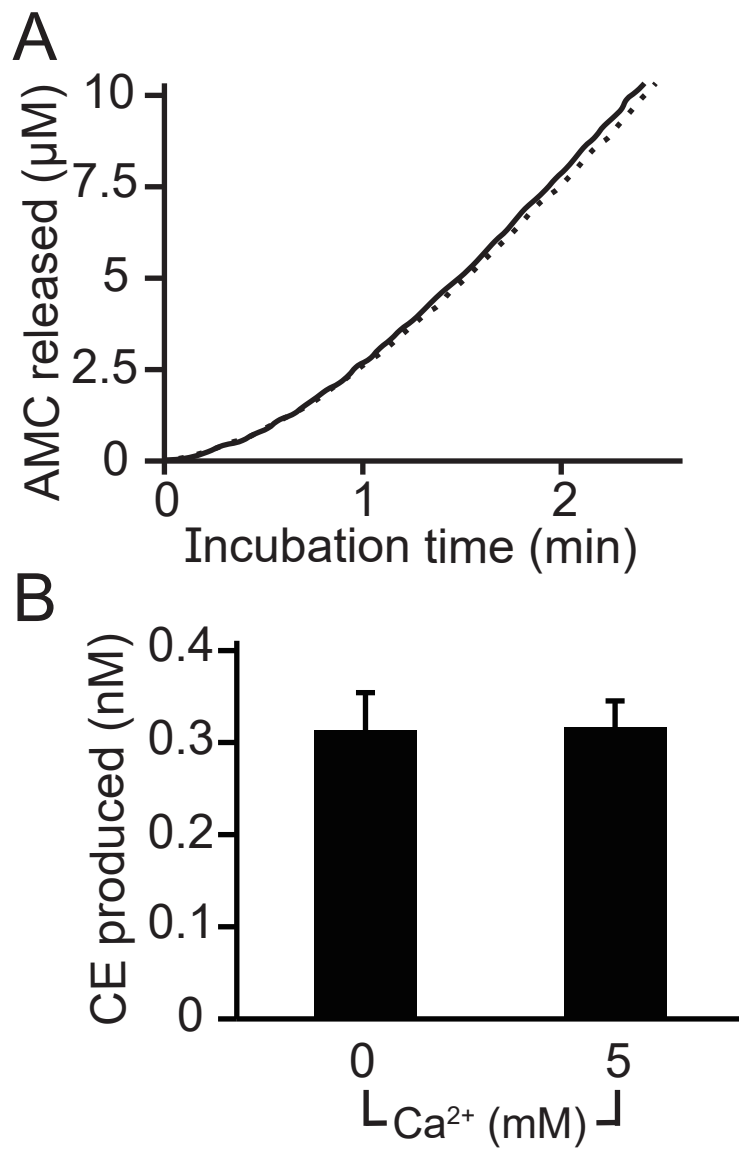
Figure 5

Figure 6

Figure 7

A

B

Tt-proC (805-816)	−GKYYRDDSRDD**D**−
Tt-proB (188-197)	−GGHYIKR−−GQ**E**−
Tt-proCE (164-173)	−G**E**HNLYS−−TD**D**−
Tt-proG-beta (108-119)	−GAHDIDNSGTNY−
Hd-PPAF-Ⅱ (217-226)	−G**E**WDTLT−−EK**E**−
Dm-Grass (178-187)	−G**E**HRIST−−EE**D**−
Hs-Faxtor-Ⅸ (275-286)	−G**E**HNIEETEHT**E**−
Hs-Factor-Ⅶ (269-280)	−G**E**HDLSEHDGD**E**−
Bt-trypsinogen (74-85)	−G**E**DNINVVEGN**E**−

70   80

⌐ 70-80 ⌐
    loop

Figure 8

ProC

ProB

ProCE

Figure 9

121
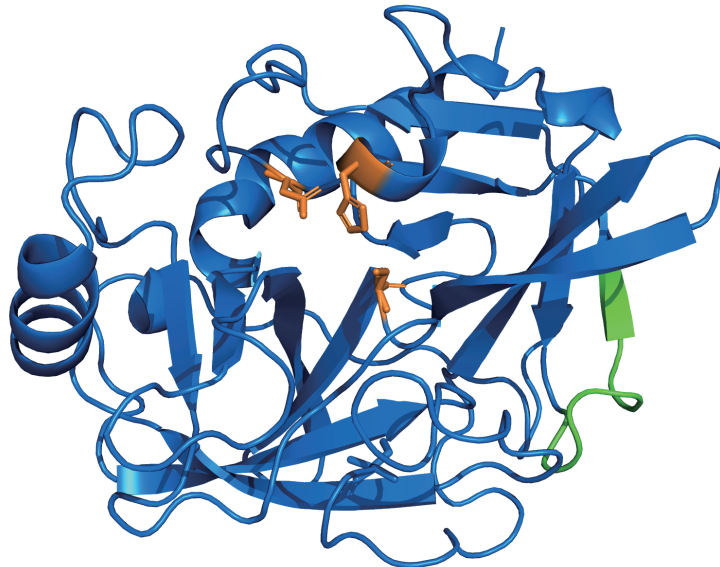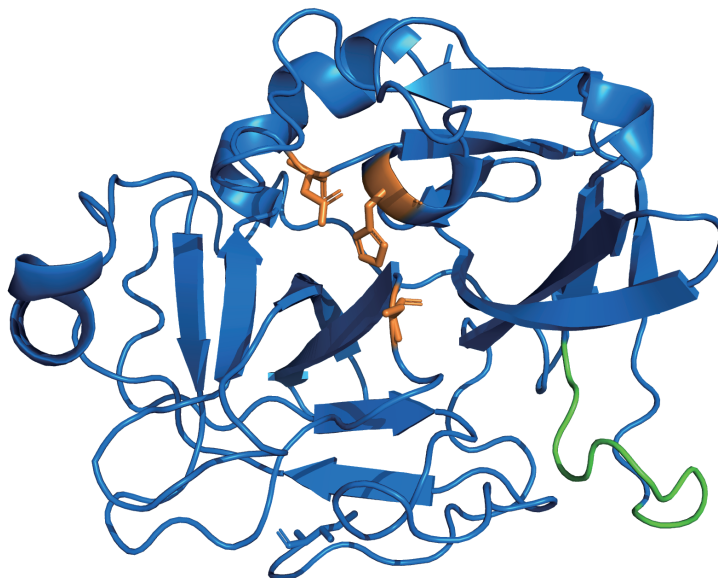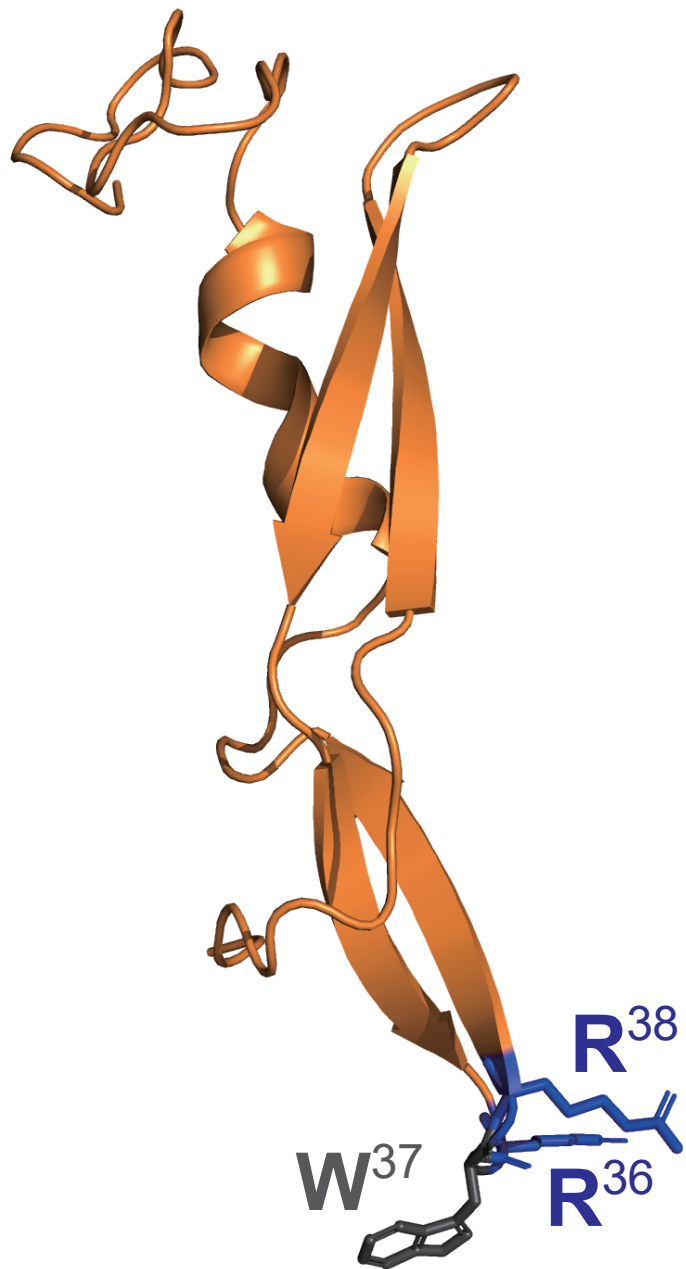
Cys-rich domain of proC

Clip domain of proB

122

Figure 10

LPS

LPS + Ca²⁺
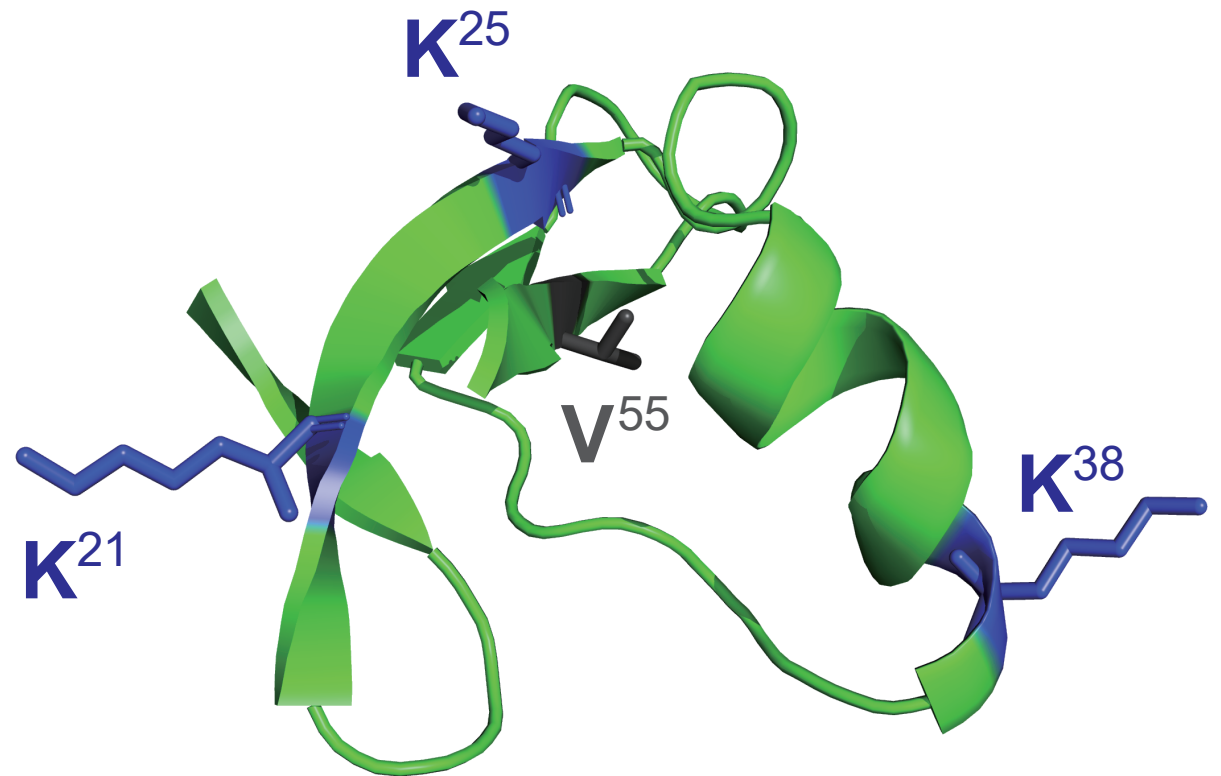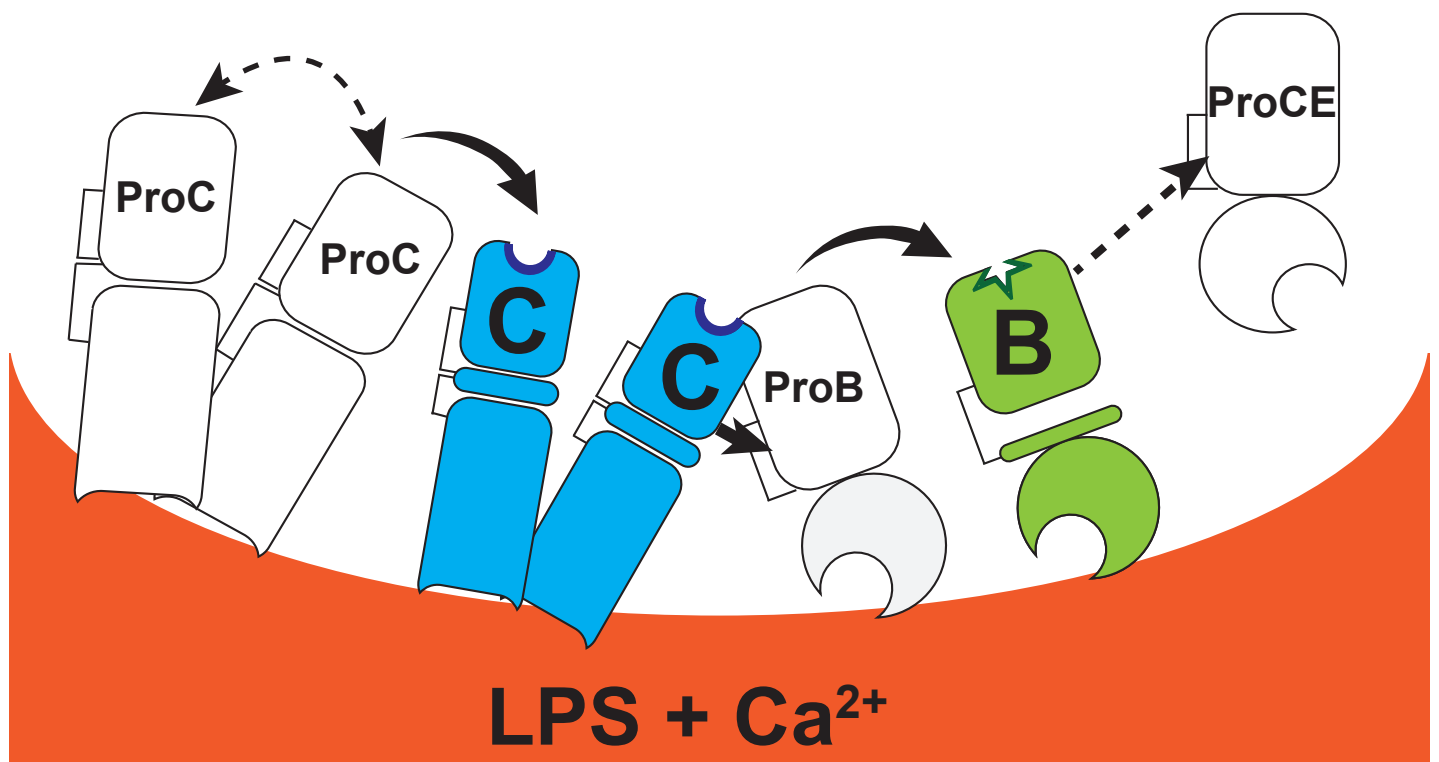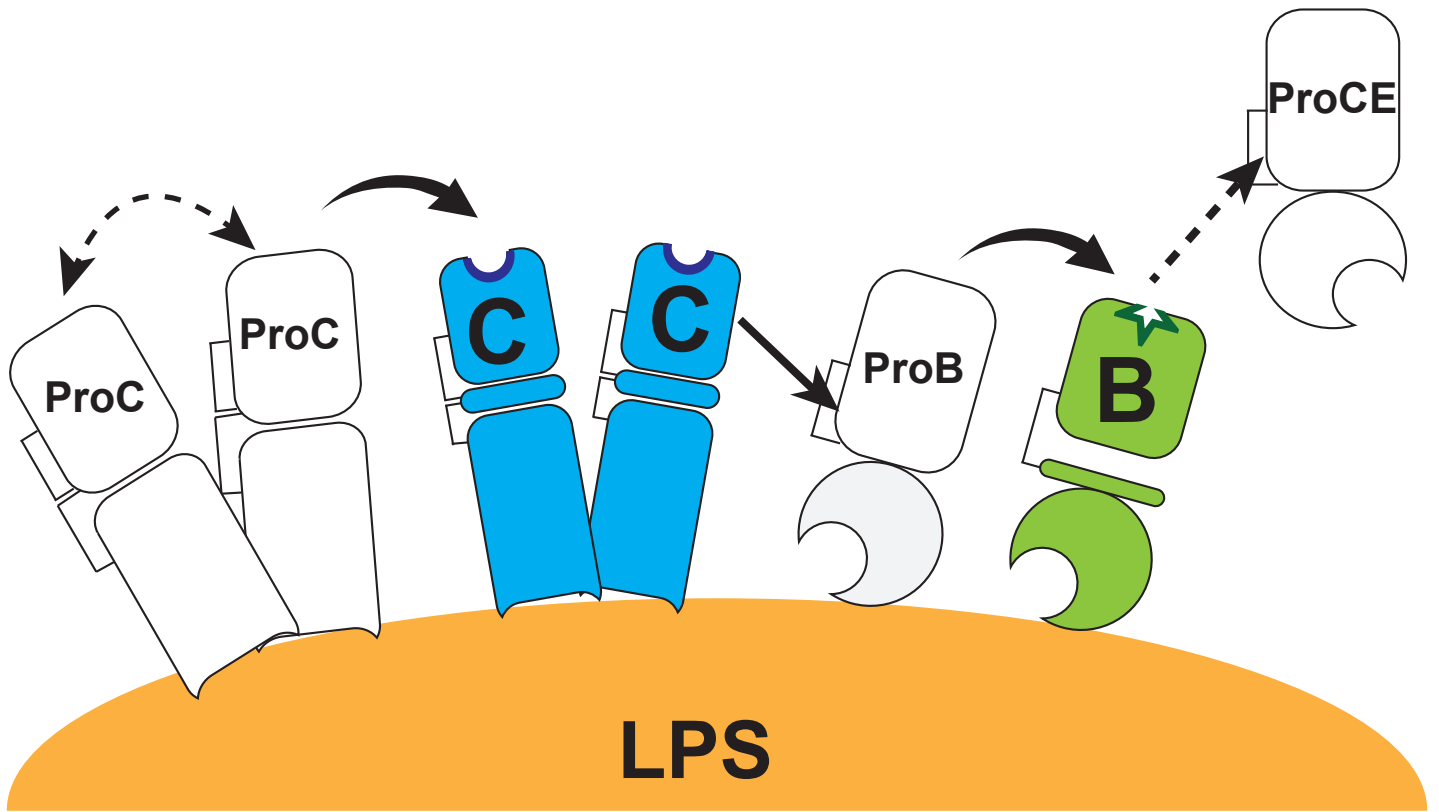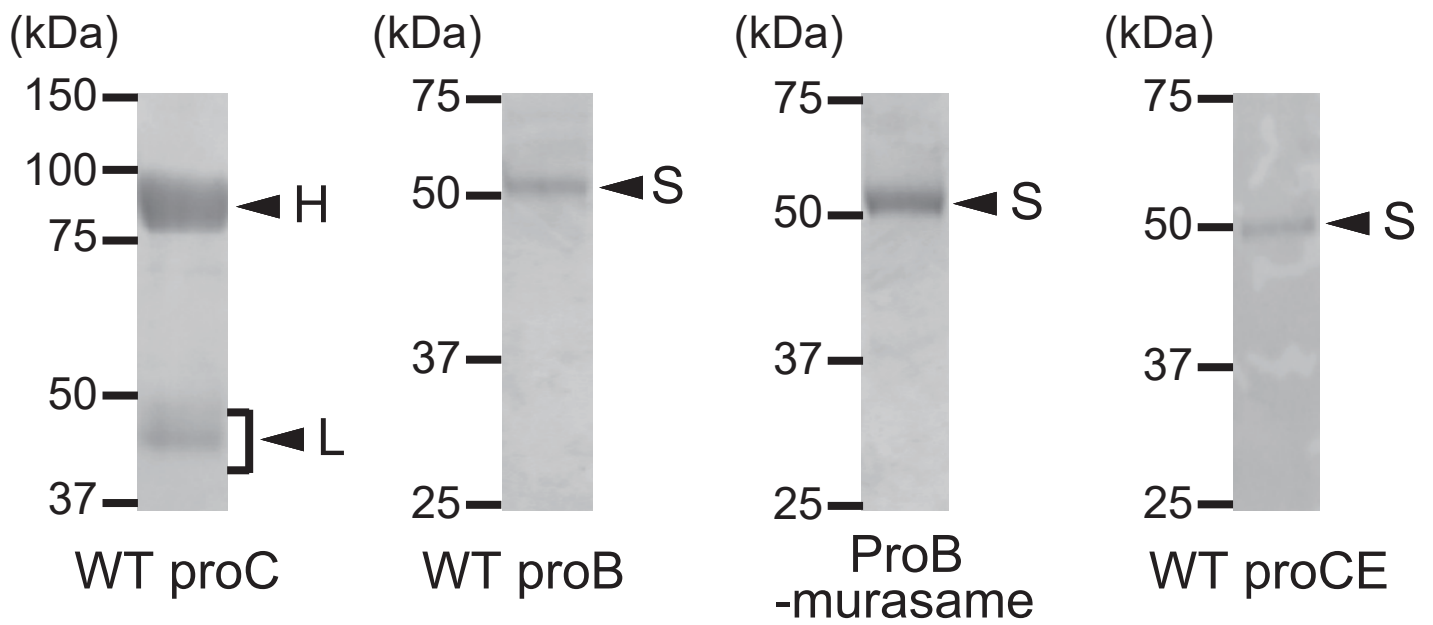
Figure 11

Supplemental Figure S1

Trypsinogen
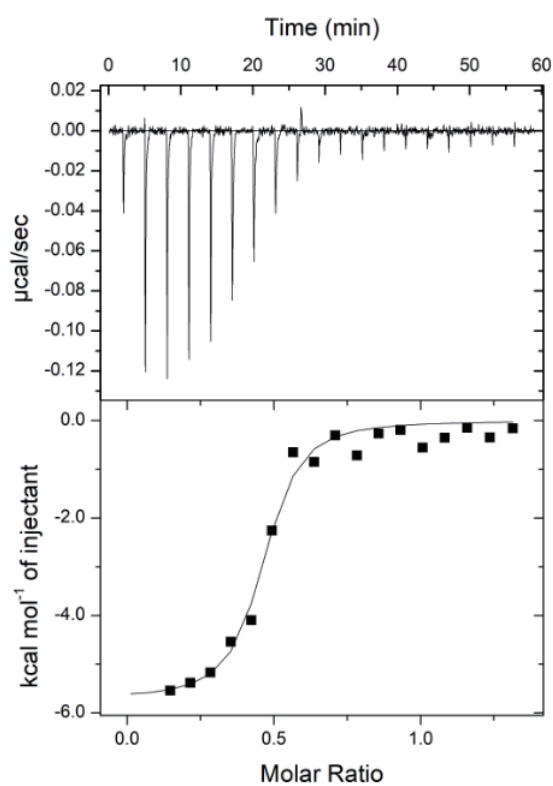
WT proC
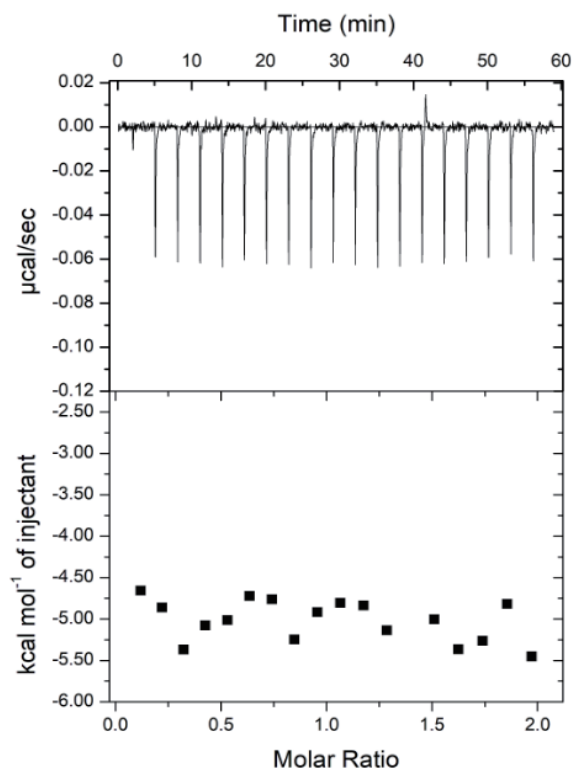
ProB
-murasame
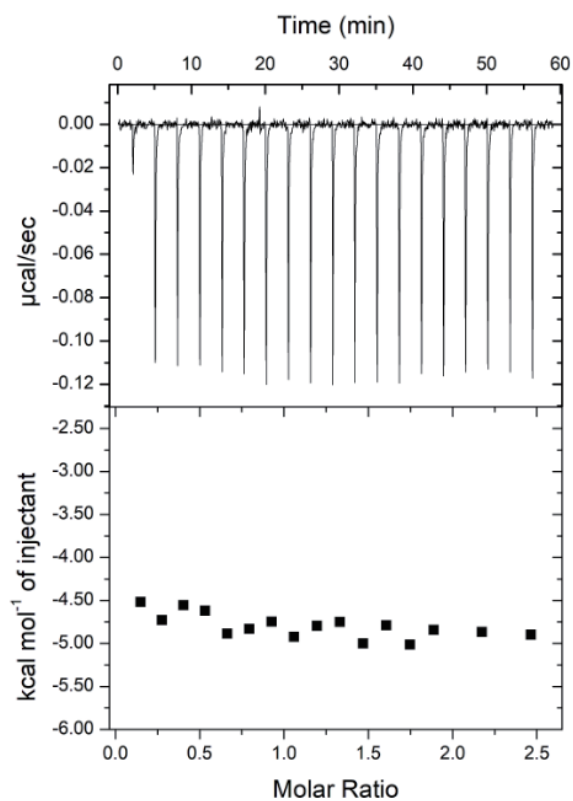
WT proCE
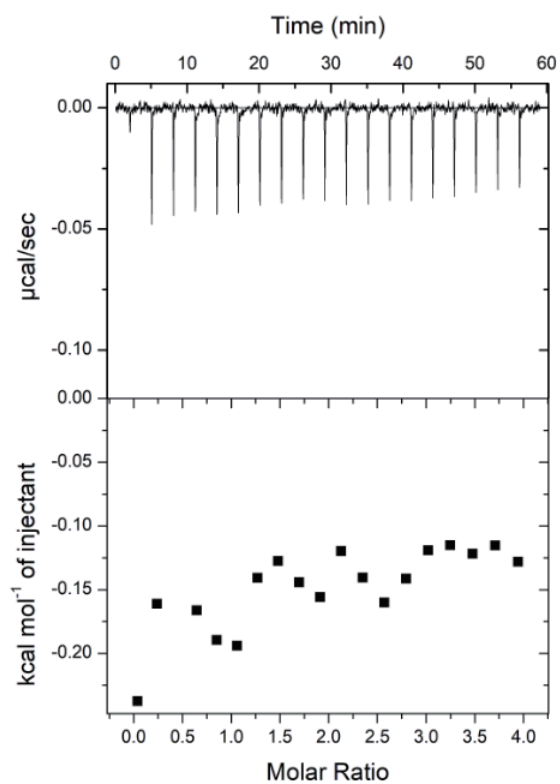
Supplemental Figure S2

Acknowledgements

Studies described in the present thesis have been carried out under the cordial guidance of Professor Dr. Shun-ichiro Kawabata (Faculty of Science, Kyushu University) for 6 years. Professor consistently taught me how to think and evaluate in biochemistry. In retrospect, my study in Kyushu University has been a series of difficulties and miracles. Although Professor never gave me clear answers about these situations, Professor always seemed to give me hints on how to overcome difficult situations. I believe one of the answers is to take care well of the people around me, communicate well with them, and thank them. The study about coagulation factors of horseshoe crabs has a very small population of researchers worldwide, but I learned not only about technical methodology but also about the basics of promoting biochemical research from this joint study under the Professor's guidance.